Progress in Surface Science 98 (2023) 100705

Contents lists available at ScienceDirect

Progress in Surface Science

journal homepage: www.elsevier.com/locate/progsurf

Review article

Floquet engineering of topological states in realistic quantum materials via light-matter interactions

Hang Liu [a,b,1], Haijun Cao [a,c,1], Sheng Meng [a,b,c,*]

[a] Beijing National Laboratory for Condensed Matter Physics and Institute of Physics, Chinese Academy of Sciences, Beijing 100190, China
[b] Songshan Lake Materials Laboratory, Dongguan, Guangdong 523808, China
[c] University of Chinese Academy of Sciences, Beijing 100049, China

ARTICLE INFO

Keywords:
Light-matter interaction
Quantum material
Floquet-Bloch topological electronic state
Nonequilibrium band structure
First-principles calculation

ABSTRACT

Electronic states in quantum materials can be engineered by light irradiation, which is greatly advanced by ab-initio computational predictions in realistic light-matter coupled systems. Here we review the most recent progresses from first principles computation in the light-driven Floquet steady states and transient dynamical states with topological electronic bands in real crystals. We first introduce the first-principles modeling approach, dubbed time-dependent Wannier scheme, for simulating real quantum materials under light irradiation. Then, we present a few examples of theoretically-predicted Floquet-Bloch electronic bands engineered by time-periodic light fields, which include the three types of Floquet-Dirac fermions in graphene and black phosphorus, the Floquet-Chern flat bands with an unprecedented high flatness ratio of band width over band gap in a Kagome material, and the Floquet conversion between bright and dark valley excitons in monolayer transition-metal dichalcogenides. Next, we show the ultrafast dynamical evolution of Weyl nodal points in orthorhombic WTe_2 driven by a time-aperiodic short light pulse, and discuss the connection between the Floquet and transient states engineered by light. After that, we introduce three prominent experiments, inspired by theoretical predictions, on the light-induced topological Floquet electronic bands in quantum crystalline materials. Finally, we make a brief summary and perspective on the engineering of topological electronic states through light-matter interactions.

1. Introduction

Quantum materials can interact with external light fields to give rise to Floquet steady states and transient dynamical states, driven by time-periodic prolonged fields and time-aperiodic ultrashort fields, respectively. The transient states, evolving with time, exist in a flash [1–3]. While the Floquet states exist for a duration in time [4,5], whose persistent nature is intriguing for us to create and control new states of matter by light irradiation. Crystalline materials with the Floquet states can be depicted by time-independent Hamiltonians, indicating the light-matter coupled systems are in steady states [6–10]. Owing to absorption and emission of photons, infinite replica electronic bands form in Floquet energy spectra of the steady states, where time periodicity endows the spectra with an

* Corresponding author at: Beijing National Laboratory for Condensed Matter Physics and Institute of Physics, Chinese Academy of Sciences, Beijing 100190, China.

E-mail address: smeng@iphy.ac.cn (S. Meng).

[1] The authors contribute equally to this work.

https://doi.org/10.1016/j.progsurf.2023.100705

Available online 23 April 2023

effective Brillion zone (BZ) in energy space, resembling the reciprocal BZ resulted from space periodicity of crystal structures. Importantly, the resultant Floquet-Bloch bands are not just photon-dressed replicas of equilibrium electronic bands; instead, the bands could be reshaped by coherent light-matter interactions. Thus, shining time-periodic light emerges as an effective approach for the flexible engineering of electronic properties of matter in the Floquet steady states.

The band reshaping via time-periodic light illumination enables a great potential to control electronic topology in quantum materials. In band structures, degeneracy of nodal points can be lifted and conventional energy gaps can be inverted to create Floquet topological insulators, resulted from light-induced effective spin–orbit coupling (SOC) [11–29]. As an intriguing phase of matter, the topological insulator exhibits insulating bulk and conducting helical edge states, which would give rise to the quantum spin Hall effect that is immune to perturbations. The Floquet insulating gaps with topology can also be induced from avoided crossings of photon-dressed replica bands due to energy level repulsion, rooted in the optical Stark effect [21–23,26–37]. With a similar mechanism, the Floquet insulators with Chern gaps and energy valleys have also been revealed to be controlled by time-periodic light [38–47]. The chiral edge state of Chern insulator, with a spin channel of topological insulator, supports quantum anomalous Hall effect.

Furthermore, gapless quasiparticles from band crossings can be created, transformed, and destroyed in both the original and photon-dressed electronic bands of Floquet semimetals with Weyl, Dirac, nodal-line, and nodal-ring fermions [48–62]. The nodal points of a Weyl semimetal have two-fold band degeneracy, and a pair of the Weyl points with the opposite monopole charges can merge to form a Dirac semimetal with four-fold band degeneracy at nodal points. To characterize electronic band topology of these Floquet states, theories have been developed [63–77], in which some formulations, such as the Floquet Chern numbers calculated by integrating Berry curvature over the first Brillouin zone, and the Floquet winding numbers rooted in the time-evolution operator within a single driving period [63], are distinguished from that of the ground state.

To realize Floquet band topology, ab-initio theoretical calculations have predicted novel properties in realistic light-matter coupled systems, where some of them have been confirmed in pump–probe experiments. Floquet topological and Chern insulators are proposed in graphene and FeSe with tunable SOC driven by circularly polarized light (CPL) [78,79], and Floquet valley polarization from the optical Stark effect is proposed in the driven transition-metal dichalcogenides (TMDs) [80,81]. Experimentally, massive Floquet-Dirac states have been observed by measuring time- and angle-resolved photoemission spectroscopy (tr-ARPES) for driven surface states of Bi_2Se_3 [82–84]. The anomalous Hall effect from the Floquet-Chern states was confirmed by electronic transport measurement in CPL-driven graphene [85]. In addition, the Floquet control of energy valleys in TMDs was shown by detecting optical absorption of electrons [86–89]. However, the gapless Floquet-Weyl and Floquet-Dirac semimetals, respectively predicted to exist in Na_3Bi with light-broken time reversal symmetry [90] and in black phosphorus (BP) with optical Stark effects [91], are to be experimentally verified. These realistic light-matter coupled Floquet systems, from the ab-initio predictions and experimental observations, are less popular than enormous proposals from theoretical toy models, indicating ab-initio and experimental studies need to be further developed. Despite this fact, all these studies demonstrate that the electronic topology in quantum materials can be flexibly engineered by time-periodic Floquet light driving to achieve controlled topological states.

In contrast to the Floquet steady states [4,5], irradiating a short time-aperiodic light pulse is a way to dynamically engineer transient nonequilibrium states of matter in a flash [1–3]. For examples, Weyl fermions can be transiently controlled with dynamical evolution behaviors [92,93], and photoinduced room-temperature superconductors can exist in several picoseconds to a few nanoseconds [94,95]. By extending light pulses to be long enough, time periodicity can be approximately reached to induce Floquet states, as in the pump–probe experiments for achieving both the topologically nontrivial states mentioned above and the topologically trivial states [96–98]. Hence, Floquet engineering may be a new window to stabilize transient states, such as the realization of light-induced persistent superconductivity [99].

Overall, light illumination is an effective way of controlling topological states in crystals, where the realistic predictions from theoretical studies drive materials engineering forward by laying down a foundation for experiments. Therefore, this article reviews our recent progresses in ab-initio theoretical predictions of light-induced topological states, focusing on the Floquet electronic states in

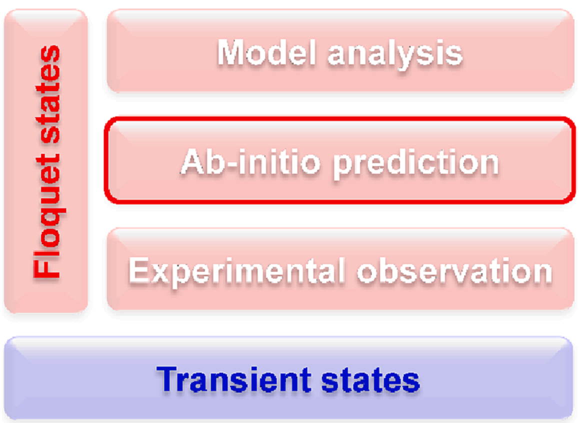

Fig. 1. Research categories on light-induced nonequilibrium states. This review article focuses on ab-initio theoretical predictions of the Floquet topological electronic states in real crystalline materials.

crystalline materials (Fig. 1). The article is organized as follows: Section 2 shows the computational methodology for modeling realistic light-driven crystals; then, Section 3 presents the Floquet light engineering of Dirac fermions, energy valleys, and flat bands (FBs) in multiple layered quantum materials; next, Section 4 introduces the controlled transient Weyl fermions under time-nonperiodic light fields; afterwards, Section 5 shows three experiments on observing topological Floquet-Bloch states; and finally, Section 6 presents a short summary and perspective on the Floquet engineering of topological electronic states through light-matter interactions.

2. Methodology

In this section, we review theoretical formalisms and computational methods for simulating the electronic states in real crystalline solids driven by external light fields.

2.1. Time-dependent Bloch Hamiltonian

Crystalline solids can be described by the Bloch Hamiltonian $H(\boldsymbol{k})$ with crystal momentum $\boldsymbol{k}$. Under light irradiation, the Hamiltonian becomes time-dependent by Peierls substitution

$$H(\boldsymbol{k})\rightarrow H(\boldsymbol{k},t) = H(\boldsymbol{k}+\boldsymbol{A}(t)), \tag{1}$$

where the gauge-invariant vector potential $\boldsymbol{A}(t)$ with time t describes the applied light field. The electronic states in light-driven crystals are determined through the Schrödinger equation

$$i\frac{\partial}{\partial t}|\psi(\boldsymbol{k},t)\rangle = H(\boldsymbol{k},t)|\psi(\boldsymbol{k},t)\rangle. \tag{2}$$

Here, the time-dependent Hamiltonian $H(\boldsymbol{k},t)$ treats quasiparticle interactions within crystals quantum mechanically and light fields classically, which is suitable for all the studies expounded in this review article.

2.2. Time-independent Floquet-Bloch Hamiltonian

For a time-periodic light field $\boldsymbol{A}(t) = \boldsymbol{A}(t+T)$ with the period of T, the time-dependent Hamiltonian is also periodic in time, expressed as

$$H(\boldsymbol{k},t) = H(\boldsymbol{k},t+T). \tag{3}$$

Due to the time periodicity, Floquet theorem can be applied to solve Eq. (2), where the time-dependent electronic wavefunction $|\psi(\boldsymbol{k},t)\rangle$ is formulated as [6–10]

$$|\psi(\boldsymbol{k},t)\rangle = e^{-i\varepsilon(\boldsymbol{k})t}|\Phi(\boldsymbol{k},t)\rangle \text{ with } |\Phi(\boldsymbol{k},t)\rangle = |\Phi(\boldsymbol{k},t+T)\rangle. \tag{4}$$

Expanded in discrete Fourier series, the time-periodic auxiliary function $|\Phi(\boldsymbol{k},t)\rangle$ is

$$|\Phi(\boldsymbol{k},t)\rangle = \sum_n e^{-in\omega t}|u^n(\boldsymbol{k})\rangle, \tag{5}$$

where $\omega = 2\pi/T$ is the light frequency, and $n \in (-\infty, +\infty)$ is an integer. As a result, the Equation (2) with time dependence is transformed into a time-independent equation

$$\sum_n H_{mn}(\boldsymbol{k})|u^n(\boldsymbol{k})\rangle = (\varepsilon(\boldsymbol{k}) + m\hbar\omega)|u^m(\boldsymbol{k})\rangle, \tag{6}$$

where $H_{mn}(\boldsymbol{k}) = \frac{1}{T}\int_0^T H(\boldsymbol{k},t)e^{i(m-n)\omega t}dt$. In matrix form, the cascaded equation is written as

$$\begin{bmatrix} \ddots & \vdots & \vdots & \vdots & \iddots \\ \cdots & H_{-1,-1}(\boldsymbol{k})+\hbar\omega & H_{-1,0}(\boldsymbol{k}) & H_{-1,1}(\boldsymbol{k}) & \cdots \\ \cdots & H_{0,-1}(\boldsymbol{k}) & H_{0,0}(\boldsymbol{k}) & H_{0,1}(\boldsymbol{k}) & \cdots \\ \cdots & H_{1,-1}(\boldsymbol{k}) & H_{1,0}(\boldsymbol{k}) & H_{1,1}(\boldsymbol{k})-\hbar\omega & \cdots \\ \iddots & \vdots & \vdots & \vdots & \ddots \end{bmatrix} \begin{bmatrix} \vdots \\ |u^{-1}(\boldsymbol{k})\rangle \\ |u^{0}(\boldsymbol{k})\rangle \\ |u^{1}(\boldsymbol{k})\rangle \\ \vdots \end{bmatrix} = \varepsilon(\boldsymbol{k}) \begin{bmatrix} \vdots \\ |u^{-1}(\boldsymbol{k})\rangle \\ |u^{0}(\boldsymbol{k})\rangle \\ |u^{1}(\boldsymbol{k})\rangle \\ \vdots \end{bmatrix}, \tag{7}$$

where the time-independent square matrix with infinite dimensions is dubbed as Floquet-Bloch Hamiltonian $H_F(\boldsymbol{k})$. Its eigenvalue $\varepsilon(\boldsymbol{k})$ and eigenvector $|u(\boldsymbol{k})\rangle$ are the energy and wavefunction of light-induced Floquet-Bloch electronic states, where the relation between ε and $\boldsymbol{k}$ is dubbed Floquet-Bloch band structure.

As an attribute, time periodicity renders the Floquet bands with an effective BZ ranging from $-\hbar\omega/2$ to $+\hbar\omega/2$ in energy space. This shows that the $\varepsilon(\boldsymbol{k}) \pm |n|\hbar\omega$ would be an eigenvalue if $\varepsilon(\boldsymbol{k})$ is an eigenvalue, where the dressed replica bands originate from virtual photon processes, i.e., absorption and then reemission of $|n|$ photons and vice versa. Both the dressed ($n \neq 0$) and original ($n = 0$) bands can interact with each other to give rise to band deformations, known as optical Stark effect. The effect is encoded into the

Hamiltonians of $H(\boldsymbol{k}, t)$ and $H_F(\boldsymbol{k})$ through the Peierls substitution expressed in Eq. (1) [100]. With increasing light intensity, the deformations of Floquet-Bloch bands (i.e., optical Stark effect) would become stronger to consecutively induce different phases of electronic states; meanwhile, the electron population of $n \neq 0$ bands and originally occupied $n = 0$ bands would be raised and descended, respectively. The electron population of Floquet-Bloch bands can also be influenced by the intraband currents from light-induced electron scattering in a single cycle time scale [101], which is not considered in the theoretical simulation of tr-ARPES in Section 2.3. The BZ in energy space is analogous to the BZ in reciprocal $\boldsymbol{k}$ space resulted from space periodicity.

When the time-periodic light driving is weak and off-resonant, Floquet-Bloch Hamiltonian can be approximated by a Magnus expansion in perturbation theory [10,102]

$$H_F(\boldsymbol{k}) = H_{0,0}(\boldsymbol{k}) + \frac{1}{\hbar\omega}\left[H_{0,-1}(\boldsymbol{k}), H_{0,1}(\boldsymbol{k})\right] + \cdots, \tag{8}$$

where the commutation terms represent virtual photon processes. Note, this formulation is not suitable for on-resonant and strongly-driven Floquet-Bloch systems. In contrast, with a large truncation order of square matrix, the Equation (7) can accurately describe all types of Floquet-Bloch systems. Overall, the nonequilibrium steady states in crystalline materials under time-periodic light fields can be depicted by time-independent Floquet-Bloch Hamiltonians.

2.3. Floquet-Wannier scheme

To quantitively simulate real light-matter coupled systems, ab-initio calculations based on density functional theory can be used [91]. As shown in Fig. 2, the ab-initio calculations for equilibrium materials are first carried out to get Bloch Hamiltonians $H^W(\boldsymbol{k})$ in the basis of Wannier functions, which can be conducted by using the Vienna Ab-initio Simulation Package (VASP) with a Wannier90 interface [103,104]. Based on Eq. (1), the materials under light illumination are modelled by time-dependent Hamiltonians $H^W(\boldsymbol{k},t) = H^W(\boldsymbol{k} + \boldsymbol{A}(t))$. The excited-state Hamiltonian $H^W(\boldsymbol{k}, t)$ contains all the information on light-electron interactions and consequent phenomena, where all relevant physical observables, including that for virtual and real excited electronic states, can be computed for light-driven crystalline materials. Depending on light duration, two types of theoretical simulations are presented here for real materials, including the simulation of Floquet-Bloch electronic bands and the simulation of tr-ARPES, driven by time-periodic and -nonperiodic (i.e., pulsed) light fields, respectively.

Under time-periodic light driving, the Hamiltonian with time periodicity $H^W(\boldsymbol{k},t) = H^W(\boldsymbol{k},t+T)$ is transformed into a time-independent Floquet Hamiltonian $H_F^W(\boldsymbol{k})$, which has two formulations expressed in Eqs. (7) and (8). As a dominant quantity, Floquet-Bloch band structure is acquired by calculating the eigenvalues and eigenfunctions of $H_F^W(\boldsymbol{k})$, from which light-driven electronic topology can be characterized via band topology theory, e.g., calculating topological invariants, identifying surface or edge states, and determining transport properties. Beyond effective toy models, the Floquet-Wannier modeling scheme described here, combining density functional theory calculations with Floquet theorem, can predict the specific light-matter systems in the real world for creating and controlling Floquet steady states in nonequilibrium.

In experiments, light fields are always pulses without perfect time periodicity, but Floquet-Bloch states can still be realized by using long-duration pulses, in which time periodicity is approximately reached. The specific experimental setups can be theoretically

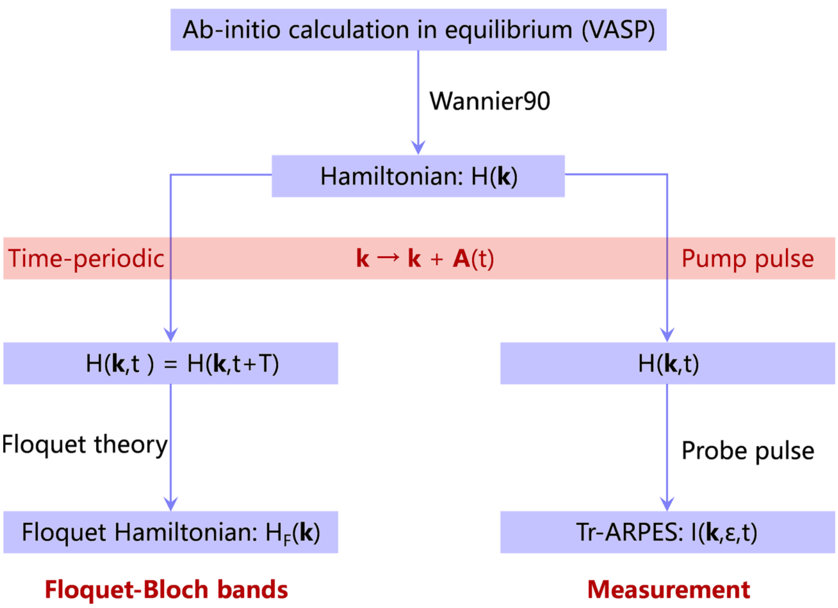

Fig. 2. Ab-initio theoretical methods for simulating light-driven Floquet-Bloch electronic states in quantum materials.

designed through simulating tr-ARPES, in which pump and probe pulses are to induce and detect Floquet states, respectively. With the Hamiltonian $H^W(\boldsymbol{k}, t)$, tr-ARPES simulations are for realistic light-matter coupled systems. The photocurrent intensity $I(\boldsymbol{k}, \varepsilon, \Delta t)$ for the wave vector $\boldsymbol{k}$, binding energy ε, and pump–probe delay time Δt is [23,105,106]

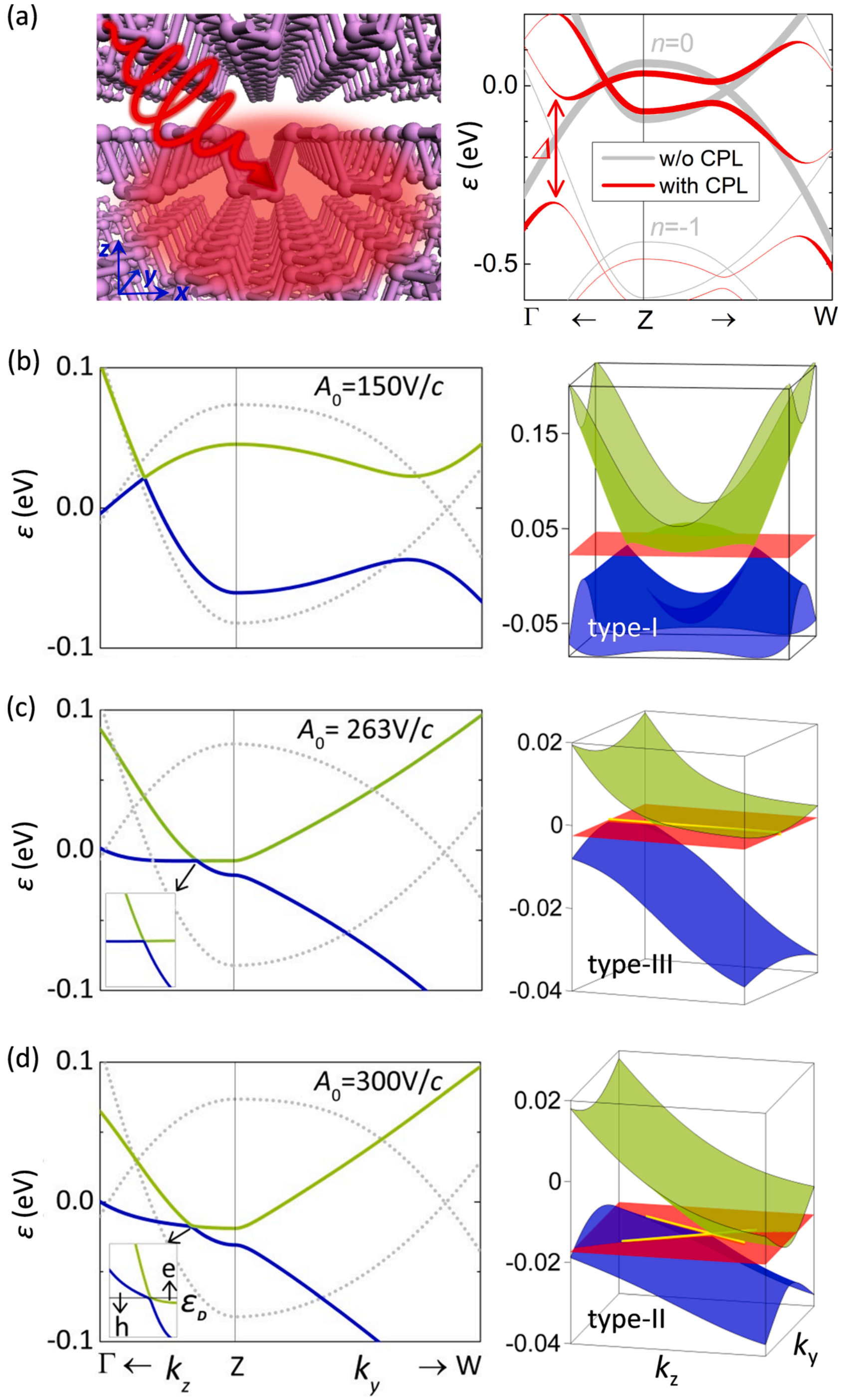

Fig. 3. Floquet-Dirac fermions in the compressed BP driven by CPL. (a) Schematic illustration of light-irradiated BP (left panel) and Floquet band structure (right panel). (b–d) Type-I, type-III, and type-II Floquet-Dirac cones induced by the CPL $\boldsymbol{A}(t) = A_0(\cos(\omega t), \sin(\omega t), 0)$ with photon energy $\hbar\omega = 0.5$ eV, and amplitude $A_0 = 150$ V/c, 263 V/c, 300 V/c, respectively. Gray dotted lines in left panels show equilibrium electronic structures. Yellow lines in right panels represent Fermi surfaces. Adapted from [91]. (For interpretation of the references to colour in this figure legend, the reader is referred to the web version of this article.)

$$I(\boldsymbol{k},\varepsilon,\ \Delta t) = Im\sum_{a}\int dt_1\int dt_2 s(t_1,\Delta t)s(t_2,\Delta t)e^{i\omega(t_1-t_2)} \times G^{<}_{aa}(\boldsymbol{k},\varepsilon,t_1,t_2), \tag{9}$$

where $G^{<}_{aa}(\boldsymbol{k},\varepsilon,t_1,t_2)$ represents diagonal terms of the lesser Green function matrix of light-driven crystals, and s is the envelope function of probe pulse. The Green function $G^{<}(\boldsymbol{k},\varepsilon,t_1,t_2) = U(\boldsymbol{k},t_1,0)G^{<}(\boldsymbol{k},\varepsilon,0,0)U^{\dagger}(\boldsymbol{k},t_2,0)$ is computed from the ground-state lesser Green function $G^{<}(\boldsymbol{k},\varepsilon,0,0)$ and time evolution operator $U(\boldsymbol{k},t,t')$, based on the Hamiltonian $H^W(\boldsymbol{k})$ and $H^W(\boldsymbol{k},t)$, respectively. In realistic tr-ARPES experiments, electrons in Floquet states are excited to the states in vacuum, named by Volkov states, for measurement, where the two different types of light-induced states interact with each other to further change the energy levels of Floquet states [84,107,108]. This originates from the photon dressing induced by the probe pulse, which is similar to the photon processes for inducing Floquet states by the pump pulse. The influence of measurements on Floquet states is not considered in the simulation of tr-ARPES here.

With the tr-ARPES simulation, light fields suitable for experiments would be quantitatively predicted, such as the duration and envelope of pump and probe pulses (e.g., full width at half maximum for Gaussian pulses), and the delay time between pump and probe pulses. Also, by changing delay time Δt, the dynamical processes of Floquet-Bloch electronic states can be tracked with time. In addition, the transient electronic states under short-duration light pulses can be modelled from the time-dependent Hamiltonian $H^W(\boldsymbol{k},t)$ in the basis of Wannier orbitals; currently, this can also be done by using the ab-initio software of Time-Dependent Ab-initio Package (TDAP) [109] and Octopus [110], which is based on time-dependent density functional theory.

3. Engineering topological Floquet-Bloch states

Based on the Floquet-Wannier modeling scheme, three types of light-driven Floquet-Bloch topological electronic structures, including the linear Dirac bands, the parabolic energy valleys, and the non-dispersive FBs, are presented below for multiple real materials.

3.1. Floquet-Dirac fermions in black phosphorus

As a layered semiconductor [Fig. 3(a)], BP has attracted tremendous interests due to its remarkable optical/electrical properties and resultant potential applications [111–118]. In particular, strain and electric fields can invert its direct band gap into Dirac cones and nodal rings for two-dimensional (2D) and three-dimensional (3D) BP, respectively [119–124]. As an effective method to control materials, the Floquet light illumination appears to be intriguing for changing the electronic band topology of nonequilibrium BP, where exotic physical states and phenomena in driven BP have been recently found from ab-initio theoretical simulations [91].

For the 3D BP material with a 3.72% compressive strain along armchair direction, its conduction and valence bands are inverted to form a type-I Dirac nodal ring around the Fermi energy. Driven by a CPL $\boldsymbol{A}(t) = A_0(\cos(\omega t),\ \sin(\omega t),\ 0)$ propagating along stacking direction, the equilibrium nodal-ring band develops into two Dirac points, as exemplified in Fig. 3(b) for the time-periodic CPL with the photon energy $\hbar\omega = 0.5$ eV and light amplitude $A_0 = 150$ V/c (c is the velocity of light in vacuum). The light-induced Floquet-Dirac cones, with a point-shape Fermi surface, are thus classified to be type-I cones. Furthermore, the Floquet-Dirac fermions in driven BP can be controlled. As shown in Fig. 3(d), at the light field amplitude $A_0 = 300$ V/c, the Dirac cones are strongly tilted to have electron and hole pockets simultaneously at the Fermi energy, thus the Floquet-Dirac cones represent type-II fermions.

Between the type-I and type-II Floquet-Dirac cones, there is a critical state driven by the CPL with the amplitude $A_0 = 263$ V/c, where the cones lying flat at the Fermi energy exhibit a line-shape Fermi surface [Fig. 3(c)]. This manifests the formation of a new type of Dirac state, dubbed type-III Floquet-Dirac fermion. Thus, by tuning light intensity, the tilting of Floquet-Dirac cones can be engineered, in which three types of Dirac fermions and their phase transitions are induced in the CPL-driven BP. Besides, the states and transitions can be induced and controlled through tuning other parameters of light, as demonstrated in [91]. In comparison, one band of the type-III cone has the Fermi velocity of zero along a specific $\boldsymbol{k}$ path, while the two bands of type-I (type-II) cones have nonzero Fermi velocities in the opposite (same) directions. Also, due to different Fermi surfaces of the Dirac cones, the density of states approaching the Fermi energy exhibit vanishing, increasing, and finite amplitudes for the type-I, type-II, and type-III cones, respectively. The distinctions of band dispersions endow the three types of Dirac cones with different intriguing phenomena, such as the unusual magnetoresponses of type-II cones [125–128]. Interestingly, the behaviors of type-III Dirac fermions are similar to that of particles at the event horizon of a gravitational black hole (BH), showing that the light-driven BP with type-I, type-II, and type-III Dirac fermions appears to be an excellent new platform to achieve the BH analogue in materials and its Hawking radiation [129].

Mechanisms behind the controlled Dirac states in BP are revealed through analyzing light-driven processes. As shown in the right panel of Fig. 3(a), when the CPL is irradiated on BP, electrons emit and absorb $|n|$ photons to form the photon-dressed bands indexed with $n = \ldots, -2, -1, 1, 2, \ldots$ (gray thin lines); and the original band is indexed with $n = 0$ (gray bold lines). At crossing points between the $n = -1$ and $n = 0$ bands, the hybridization between the two bands lifts point degeneracy to form a gap following a linear evolution $\Delta \propto A_0$, known as the optical Stark effect. With increasing CPL intensity, the band gap Δ becomes larger, which tilts Floquet-Dirac cones to introduce the transition from type-I to type-II via type-III fermions.

3.2. Floquet-Dirac fermions in graphene

Graphene is another well-known layered quantum material with a variety of electrical, optical, and mechanical properties

[130–132]. Massless Dirac fermions render graphene with a high carrier mobility, and the enhanced SOC in graphene would give rise to topological insulating states with gapped Dirac cones [133]. Shining CPL has been known to effectively engineer SOC in graphene to achieve controllable Dirac gaps [24–29], as in the first proposal of topological Floquet-Bloch bands. By illuminating other types of light fields and considering the whole bands in the reciprocal BZ, graphene may exhibit much richer light-induced Floquet electronic phenomena [134], beyond all previous toy-model studies on time-periodically driven graphene [24–29,52,53].

Irradiated by a light field with the linear polarization along armchair direction [Fig. 4(a)], the conduction and valence Dirac bands of graphene, around the $\boldsymbol{k}$-point of M in BZ, shift down and up respectively, during which the two bands invert and cross with each other to form new Dirac points. This is exemplified by the induced type-I cones under the light field with the photon energy $\hbar\omega = 5.0$ eV and amplitude $A_0 = 900$ V/c [Fig. 4(b,c,d)]. Furthermore, when the light evolves to be with parameters of $\hbar\omega = 6.0$ eV and $A_0 = 980$ V/c, the induced Dirac cones are strongly tilted to become type-II cones, with both electron and hole pockets at the Fermi surface [Fig. 4(e,f)]. As a result, the type-I and type-II Floquet-Dirac points, with a small energy difference $\varepsilon_1 - \varepsilon_2 = 0.02$ eV, coexist in the light-

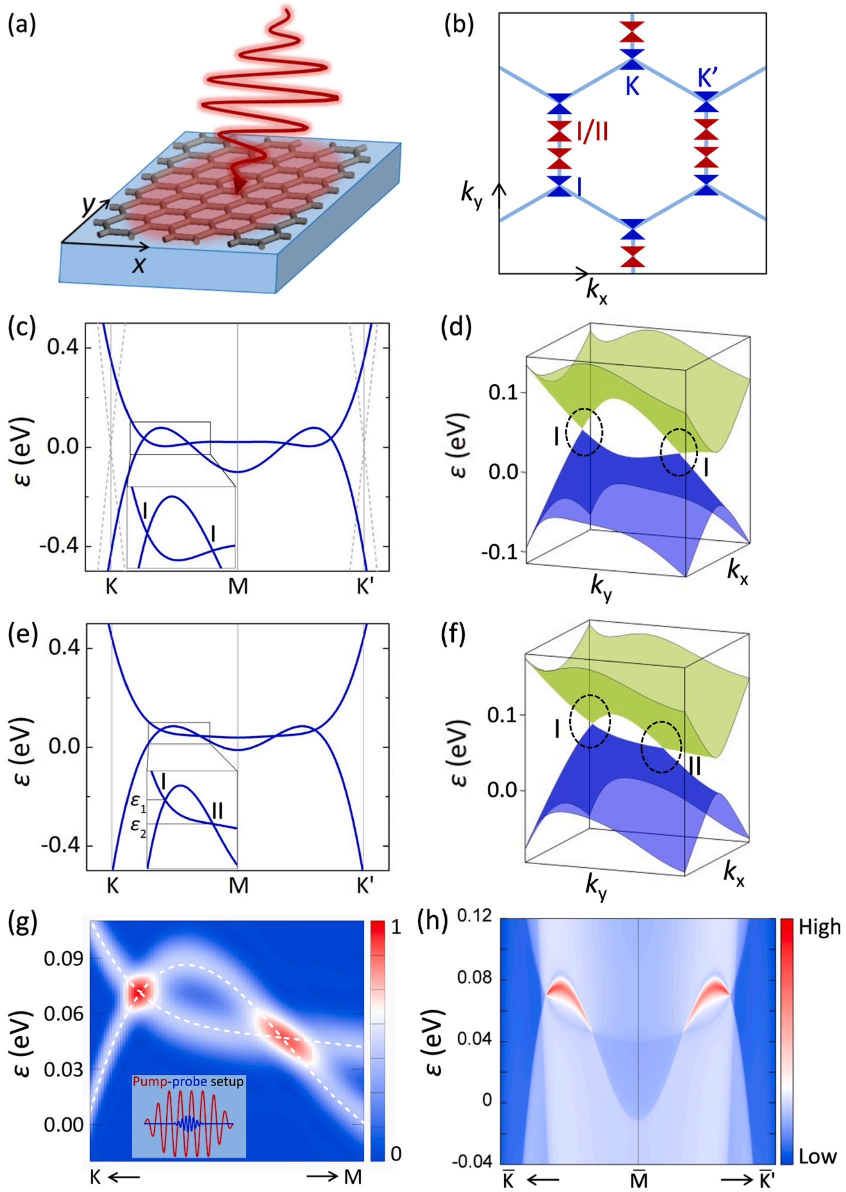

Fig. 4. Floquet-Dirac fermions in the graphene driven by linearly polarized light. (a) The field is polarized along armchair (x) direction. (b) The $\boldsymbol{k}$-space location of original (blue) and light-induced (red) Dirac cones. (c,d) Type-I cones induced by the light with photon energy $\hbar\omega$ = 5.0 eV and amplitudes 900 V/c. Dashed gray lines represent the equilibrium bands of graphene. (e,f) Type-II cones induced by the light with photon energy $\hbar\omega$ = 6.0 eV and amplitude 980 V/c. (g,h) Tr-ARPES and edge-state spectrum for the coexisting state of type-I and type-II Dirac fermions in (e,f). Adapted from [134]. (For interpretation of the references to colour in this figure legend, the reader is referred to the web version of this article.)

driven graphene. Nontrivial band topology is characterized by the edge states connecting type-I and type-II Dirac points for zigzag-terminated graphene nanoribbons [Fig. 4(h)].

Similar to that for the driven BP discussed in Section 3.1, optical Stark effects dominate the creation of both type-I and type-II Dirac points in graphene, where the downward (upward) shift of conduction (valence) Dirac band, around the $\boldsymbol{k}$-point of M, originates from the repulsion between $n = 0$ and $n = +1$ ($n = -1$) bands. As a platform with new electronic states, the light-driven graphene may be suitable for observing fascinating phenomena, such as the magnetic-field-induced Klein tunneling [135], the correlated electron-hole pairs from an analogous BH radiation [129], and the scattering between type-I and type-II Dirac quasiparticles via topological edge states.

To identify experimental setups for the light-driven graphene, tr-ARPES is simulated by using the method in Section 2.3. As shown in Fig. 4(g), the pump pulse $\boldsymbol{A}(t) = A_0p(t)(\sin(\omega t), 0, 0)$ has a trapezoidal envelope $p(t)$ with the same frequency and amplitude as that for creating coexisting type-I and type-II fermions in Fig. 4(e,f), and the probe pulse $\boldsymbol{A}(t) = A_0s(t)(\sin(\omega t), 0, 0)$ has a Gaussian envelop $s(t)$ with its peak at the middle of plateau of pump pulse. The resultant tr-ARPES agrees with Floquet-Bloch bands, in which the strongest photocurrent intensity locates at type-I and type-II Dirac points [Fig. 4(g)]. This indicates that the pump pulse with a trapezoidal envelope is a good approximation to the time-periodic continuous light fields for creating Floquet-Bloch states. Thus, the realization and observation of the coexisting type-I and type-II Dirac state in light-driven graphene is feasible in tr-ARPES experiments, in which the required ultraviolet light fields can be obtained through second-order and high-order harmonic generation [136].

3.3. Hawking radiation from Floquet-Dirac fermions

Dirac cones exhibit a similar shape to that of light cones in the relativity theory, where type-I, type-II, and type-III Dirac fermions are the analogues of particles outside, inside, and at event horizon of a Schwarzschild black hole (SBH) [137–140], as illustrated in Fig. 5(a,b). This manifests that a space-inhomogeneous system with the successively distributed type-II, type-III, and type-I fermions behaves like a SBH with analogous Hawking radiation, i.e., the electron emission from type-II to type-I region. Importantly, electrostatic interactions in solids are much stronger than gravitational forces, thus the BH analogue from topological Dirac states in crystals has a possibility to realize the BH radiation with strong intensity, characterized by an extremely high Hawking temperature T_H. Combining first-principles and quantum tunneling calculations, an analogue of strong SBH radiation is proposed in a light-driven bilayer BP with controllable Floquet-Dirac fermions [129]. This analogue is beyond the weak Hawking radiation of gravitational BHs, e.g., $T_H \sim 10^{-8}$ K for the BH with one solar mass, and all other artificial BHs, e.g., $T_H \sim 10^{-9}$ K in Bose–Einstein condensates [141–158].

Dirac fermions in 2D lattices can be described by the effective Hamiltonian $H(\boldsymbol{k}) = c_xk_x\sigma_x + c_yk_y\sigma_y + vk_y\sigma_0$, where σ_0 is identity matrix, σ_x and σ_y are Pauli matrixes, and c_y and v determine the types of Dirac fermions: $|c_y| > |v|$ for type-I, $|c_y| = |v|$ for type-III, and |

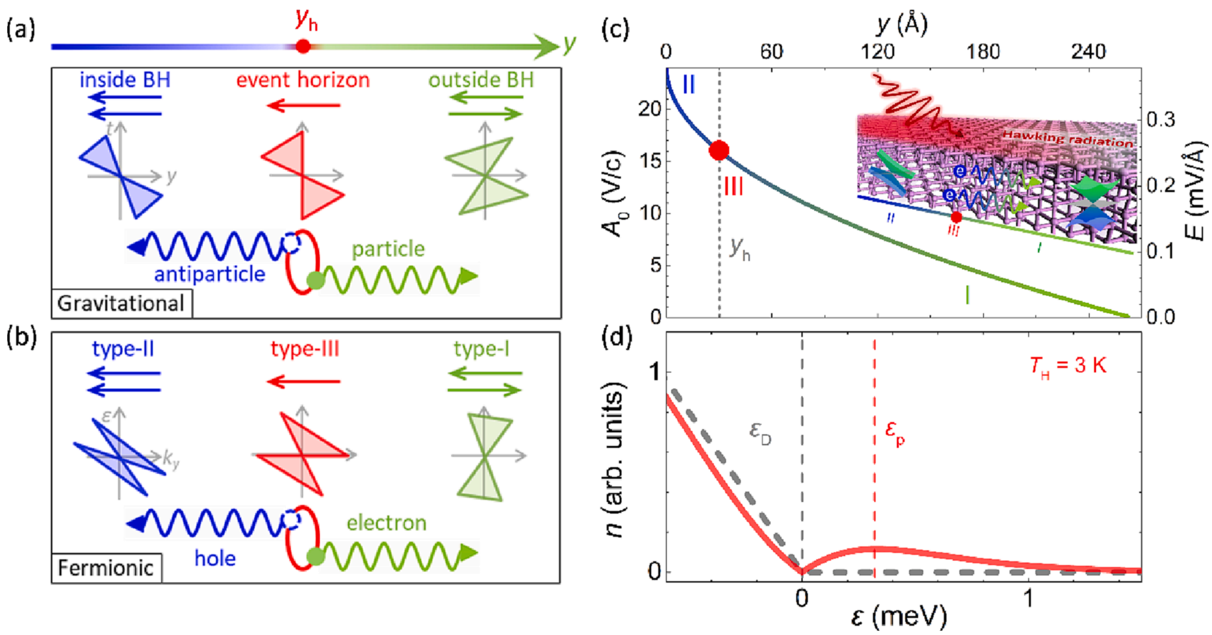

Fig. 5. Fermionic analogue of Hawking radiation in light-driven bilayer BP. (a,b) Schematic illustration of gravitational Hawking radiation, and its fermionic analogue with Dirac states in solid materials. (c,d) The theoretically designed space-inhomogeneous Floquet-Dirac states for the analogous Hawking radiation in a driven bilayer BP thin film. (c) The required distribution of light amplitude A_0 along zigzag (y) direction of BP to realize the SBH with $T_H = 3$ K. The field with linear polarization along armchair (x) direction has the photon energy $\hbar\omega = 0.03$ eV. (d) The electron population $n(\varepsilon)$ outside SBH at $y > y_h$ after the Hawking radiation with $T_H = 3$ K in the designed setup of (c). The $n_0(\varepsilon)$ before Hawking radiation is shown by the gray dashed line. Adapted from [129].

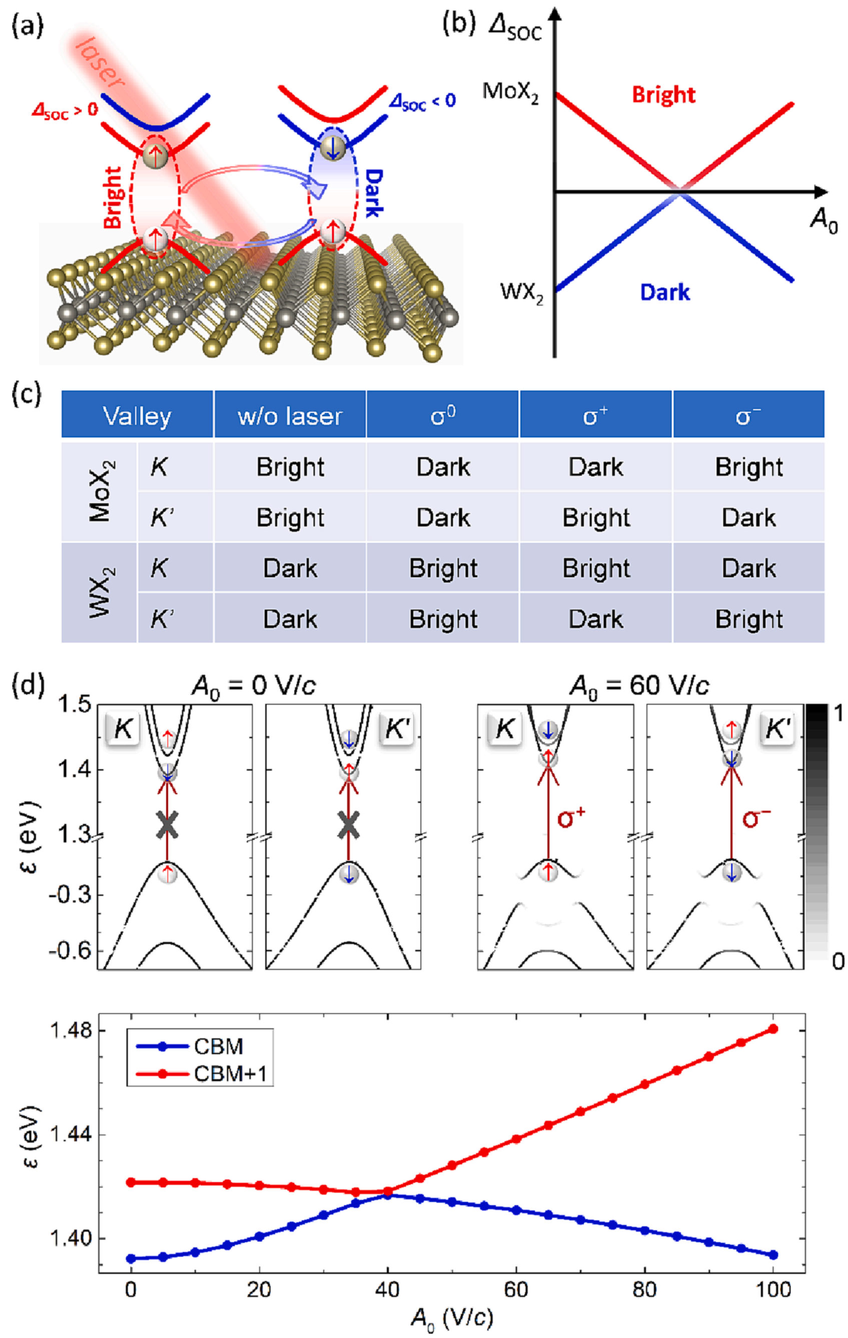

Valley		w/o laser	σ^0	σ^+	σ^-
MoX_2	K	Bright	Dark	Dark	Bright
	K'	Bright	Dark	Bright	Dark
WX_2	K	Dark	Bright	Bright	Dark
	K'	Dark	Bright	Dark	Bright

Fig. 6. Light-driven Floquet conversion of excitons in monolayer TMD materials. (a) Schematic illustration of the Floquet conversion between bright and dark excitons. (b) Illustration of light-engineered SOC gap around the CBM for the *K* valley of TMD materials. A_0 represents the amplitude of light field. (c) Possible cases of valley-dependent and light-polarization-dependent excitons conversion. σ^0, σ^+, and σ^- represent the light with linear, right-handed, and left-handed polarizations, respectively. (d) Evolution of the Floquet-Bloch bands of monolayer WS_2 (with $\Delta_{SOC} = -29.4$ meV at *K* valley) driven by a linearly polarized light field with the photon energy $\hbar\omega = 1.9$ eV. Gray level represents the weight of static ($n = 0$) component. Small arrows mark spin polarization of valley bands. Bottom panel shows the evolution of the two spin-opposite energy levels around CBM.

$c_y| < |v|$ for type-II cones, respectively. In the theory of general relativity, the Dirac Hamiltonian is represented by an effective metric

$$ds^2 = -\left(1 - \frac{v^2}{c_y^2}\right)dt^2 + \frac{1}{c_x^2}dx^2 + \frac{1}{c_y^2}dy^2 - \frac{2v}{c_y^2}dtdy, \tag{10}$$

which has the same form as that of a gravitational SBH. It shows that Dirac fermions have an effective potential energy $\Phi(y) = -\frac{1}{2}\frac{v^2(y)}{c_y^2(y)} = -\frac{1}{2}\frac{y_h}{y}$ with the required inverse proportion to distance y as that of gravitational potential, which gives rise to the distribution $c_y(y) = -v\sqrt{\frac{y}{y_h}}$. Hence, type-II fermions are inside SBH in the region of $0 < y < y_h$, type-III fermions are at event horizon $y = y_h$, and type-I fermions are outside SBH in the region of $y > y_h$ [Fig. 5(a,b)].

Based on classical kinematic equations, type-II fermions can not escape from the SBH in the region of $0 < y < y_h$. However, with quantum effects, tunneling calculations demonstrate a probability of Dirac fermions going from the type-II region inside SBH to the type-I region outside SBH, which is an analogue of Hawking radiation of gravitational SBHs. The quantum tunneling has a Planck energy spectrum $I(\varepsilon) = n^e_{\rm rad}(\varepsilon)\cdot\varepsilon$ with the number of radiated electrons

$$n^e_{\rm rad}(\varepsilon) \propto \frac{\varepsilon}{\exp\left(\frac{\varepsilon}{k_B T_H}\right) + 1}, \tag{11}$$

where k_B is the Boltzmann constant, and $T_H = \frac{1}{2\pi k_B}\left|\frac{d}{dy}(c_y - v)\right|_{y_h}$ is the Hawking temperature.

Dirac fermions for the analogous SBH can be achieved by irradiating light on a bilayer BP with Dirac cones [121]. Under a linearly polarized light field with the photon energy $\hbar\omega = 0.03$ eV, the parameter v in the BP remains unchanged, while the parameter c_y [eV·Å] $= 0.314–0.013A_0$ [V/c] decreases with light amplitude A_0, showing Dirac states in the driven BP evolve from the type-I cones with $|c_y| > |v|$ to the type-II cones with $|c_y| < |v|$ via the type-III cones with $|c_y| = |v|$. Combining the relation $c_y \sim A_0$ and spatial distribution $c_y \sim y$, the spatial distribution of light intensity would be designed to realize a space-inhomogeneous Dirac system for creating a SBH analogue and its Hawking radiation. As an example, to achieve $T_H = 3$ K, the SBH size is set at $y_h = 30.2$ Å. This requires that light amplitude decreases from 0.37 to 0 mV/Å (i.e., from $A_0 = 24.7$ to 0 V/c) in a range of 260 Å in the y (zigzag) direction of BP [Fig. 5(c)]. The well-designed setup is readily accessible in experiments. First, the high-quality crystal of 2D BP, as a familiar material, can be routinely prepared by traditional experimental approaches [119,159]. Second, the required light field with maximum amplitude of 0.37 mV/Å, photon energy of 0.03 eV, and space gradient of 1.4 μV/Å^2 is currently attainable in experiments [82,84,160].

With scanning tunneling spectroscopy or angle-resolved photoemission spectroscopy, the analogue of strong Hawking radiation would be experimentally distinguished by measuring the electron population $n(\varepsilon)$ outside SBH, i.e., in the region of $y > y_h$ [Fig. 5(d)]. The $n(\varepsilon)$ from the Hawking radiation, having Planck energy spectrum, differs from the thermally-excited Fermi-Dirac electron distribution, thus the Hawking radiation analogue can still be identified for the sample held at nonzero temperature, even above $T_{\rm H}$. Following this proposal, other systems with controllable Dirac states have also been shown to form the analogous SBH, such as the electronic materials [161,162], and artificial photonic crystals [163].

3.4. Floquet valleys in TMD materials

Layered TMD materials have energy valleys, consisting of valence band maximum (VBM) and conduction band minimum (CBM) of the direct band gaps at corners (K and K' points) of reciprocal BZ [164,165]. This enables intriguing properties in spintronics and optoelectronics, e.g., valley excitons induced by optical pumping, and valley Hall states resulted from nonzero Berry curvature [166–169]. Moreover, these properties can be engineered by tunning the valley bands. Light driving has been shown to control the energy valleys in Floquet states, such as the polarized valleys from optical Stark effects [86], and the topological energy gaps from avoided crossings between photon-dressed replicas of valley bands [80]. Below, the Floquet conversion between bright and dark valley excitons, which are respectively bound from the two states with the same and opposite spin polarizations [169], is presented for TMD materials driven by time-periodic light fields.

For monolayer TMDs, SOC splits the valley bands around CBM into spin-up and spin-down ones [170], such as $\Delta_{\rm SOC} = \varepsilon_\downarrow - \varepsilon_\uparrow > 0$ ($\Delta_{\rm SOC} < 0$) at K valley for MoX_2 (WX_2) with X = S, Se. As a result, the excitons, bound from a hole at VBM and an electron at CBM, are bright for MoX_2 (dark for WX_2) due to the same (opposite) spin polarization at the VBM and CBM. With time-periodic light driving, the optical Stark interactions, between the valley bands around CBM and the dressed $n = 1$ VBM band, change the band gap $\Delta_{\rm SOC}$, as if they were produced by an engineered effective SOC, thus giving rise to controlled valley excitons, as sketched in Fig. 6(a,b). Under the illumination of a linearly polarized light, valley bands at both K and K' valleys would be shifted through the effectively engineered SOC. At K valley, the $\Delta_{\rm SOC} > 0$ ($\Delta_{\rm SOC} < 0$) for MoX_2 (WX_2) decreases (increases) with increasing light intensity, and it becomes negative (positive) after a critical light intensity; thus, the spin splitting gap $\Delta_{\rm SOC}$ is inverted to produce the CBM and VBM with the opposite (same) spin polarization, giving rise to the dark (bright) excitons bound from a CBM-electron and a VBM-hole. This similarly takes place at light-driven K' valley with the conversion from bright (dark) to dark (bright) excitons for MoX_2 (WX_2). For instance, the VBM-CBM excitons at both the K and K' valleys in equilibrium WS_2 are dark [Fig. 6(d)]; driven by a linearly polarized light with the photon energy $\hbar\omega = 1.9$ eV and amplitude $A_0 = 60$ V/c, the spin-opposite valley bands around CBM are inverted, so the VBM and CBM after light driving have the same spin polarization to form bright excitons.

More interestingly, depending on light helicity, a CPL can selectively transform one valley, i.e., K or K' valley, of TMDs from the bright (dark) to dark (bright) excitonic state, while the other valley keeps the excitonic state as that without Floquet light driving, as summarized in Fig. 6(c). This shows that both bright and dark excitons can exist or coexist in a TMD monolayer material via Floquet engineering, and the valley-dependent and light-polarization-dependent transition between the two types of excitons can be controlled.

3.5. Floquet-Chern FBs in a Kagome material

Different from Dirac and valley bands with dispersion, the FBs without dispersion possess special intriguing properties. Chern FBs in 2D lattices have been proposed to support the Landau-level-free fractional quantum Hall effect (FQHE) at a high temperature [171–174], in which the FB is required to have a large flatness ratio, i.e., band gap (Δ) *vs.* band width (w), $\Delta/w \gg 1$. However, all the Chern FBs found so far in real materials have a small ratio $\Delta/w \sim 1$ [175–184], such as the Kagome FB in an organometallic material of $Pt_3C_{36}S_{12}H_{12}$ (HTT-Pt) [183–185]. To obtain the Chern FB with a large Δ/w in Kagome lattices, a peculiar negative kinetic hopping integral and strong SOC interactions are required, which is unlikely to be met in equilibrium materials due to the natural decay of lattice hopping integrals with the interatomic spacing. In contrast, Floquet-Chern FBs have been revealed in the CPL-driven Kagome material of HTT-Pt, with light-controlled electronic interactions, to achieve a large flatness ratio of $\Delta/w \gg 1$, and its resultant high-temperature FQHE [186].

As shown in Fig. 7(a,b), irradiated by a left-handed CPL $\boldsymbol{A}(t) = A_0(\cos(\omega t), \sin(\omega t), 0)$ with $\hbar\omega = 8\gamma_1^0$ (γ_1^0: the nearest-neighbor (NN) kinetic hopping integral for the ground state), the NN and second-nearest-neighbor (2NN) kinetic hopping integrals (γ_1, γ_2) and SOC strengths (λ_1, λ_2) for spin-up bands in monolayer HTT-Pt are modified. With the increasing light amplitude A_0, the λ_1 and λ_2 increase, and γ_2 decreases from a positive to a negative value, which is crucial to achieve a large flatness ratio Δ/w [171]. The light-engineered interactions produce an intriguing evolution of Floquet-Bloch band structures. Without light driving, the spin-up equilibrium bands possess a direct SOC gap $\Delta = 0.887\gamma_1^0$ separating the bottom Chern band with a topological number $C = -1$ and the middle Dirac band with $C = 0$ [left panel of Fig. 7(c)]; and the bottom dispersive Chern band has a width $w = 3.228\gamma_1^0$, exhibiting a quite small flatness ratio $\Delta/w = 0.27$. With light driving, the CPL with amplitude $A_0 = 800$ V/c reduces the band width of bottom Chern band to be $w = 0.022\gamma_1^0$ [right panel of Fig. 7(c)], which is ~150 times narrower than its equilibrium value. Meanwhile, the bottom band well

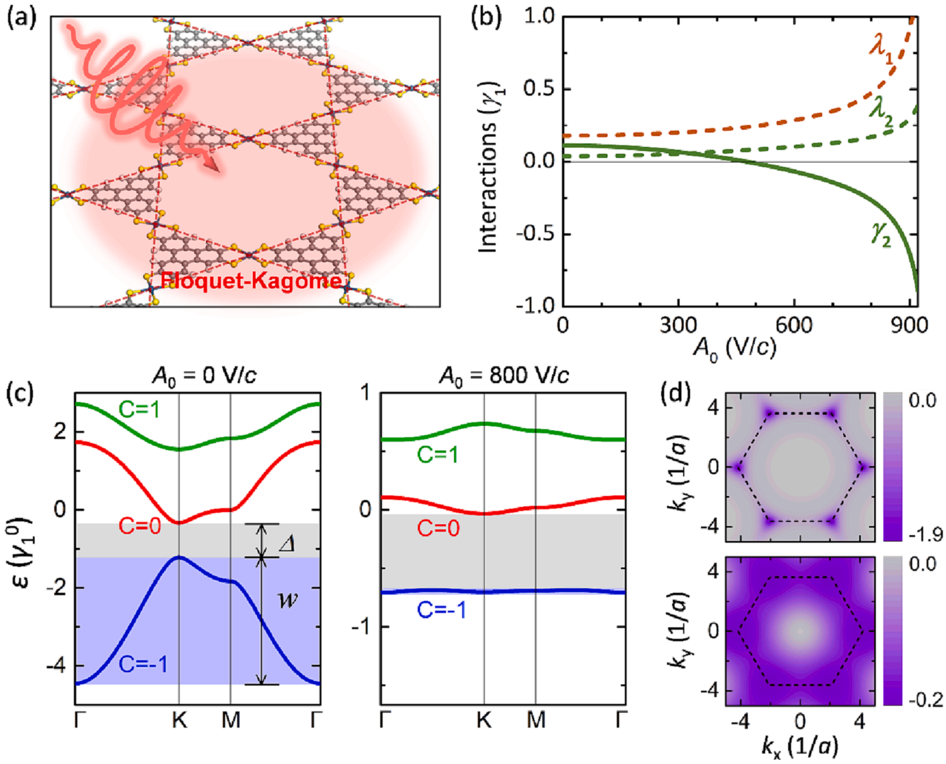

Fig. 7. Floquet-Chern FBs in a Kagome material driven by CPL. (a) Illustration of the light-driven monolayer Kagome crystal of HTT-Pt. (b) Evolution of λ_1, λ_2, and γ_2 with light amplitude A_0 for spin-up bands in HTT-Pt under the left-handed CPL with photon energy $\hbar\omega = 8\gamma_1^0$. γ_1 and γ_2 (λ_1 and λ_2) represent the NN and 2NN kinetic (SOC) hopping integrals, respectively. (c) Left panel: Kagome bands of the monolayer HTT-Pt in the equilibrium state. Right panel: Floquet-Kagome bands induced by the CPL with $A_0 = 800$ V/c in (b). (d) Top panel: Berry curvature Ω for the bottom dispersive Chern band with $\Delta/w \sim 0.27$ in the left panel of (c). Bottom panel: Light-driven Ω of the bottom Chern FB with $\Delta/w \sim 29$ in the right panel of (c). Dashed lines mark the first BZ. Adapted from [186].

separates from other bands by a large SOC gap $\Delta = 0.650\gamma_1^0$. As a result, its flatness ratio increases to an unprecedented high value $\Delta/w \sim 29$, in accordance with the light-enabled negative γ_2, and large λ_1 and λ_2.

The light-driven modification of Berry curvature (Ω) of the bottom Chern band is analyzed to identify the essential features for realizing high-temperature FQHE. At equilibrium, the Ω of the bottom dispersive Chern band is highly localized at corners (K and K' points) of the BZ [top panel of Fig. 7(d)], which is characterized by a large mean-square deviation of $\langle(\Delta\Omega)^2\rangle = 7.2 \times 10^{-2}$ [187]. Distinctively, driven by the CPL with amplitude $A_0 = 800$ V/c, Ω of the ultra-flat and isolated bottom Floquet-Chern band becomes delocalized in the whole BZ [bottom panel of Fig. 7(d)], characterized by $\langle(\Delta\Omega)^2\rangle = 3.9 \times 10^{-3}$. The uniform distribution of Ω for the FB indicates a very short magnetic length [171], which favors the FQHE with a large-size many-body excitation gap, i.e., at a high temperature [188,189]. More accurately, with the theoretical approach of exact diagonalization, one-third FQHE has been demonstrated to exist in the CPL-driven HTT-Pt at the temperature above 70 K [186].

4. Engineering transient Weyl fermions in a TMD material

Besides the Floquet steady states from time-periodic light driving, topological electronic states can also be dynamically induced and

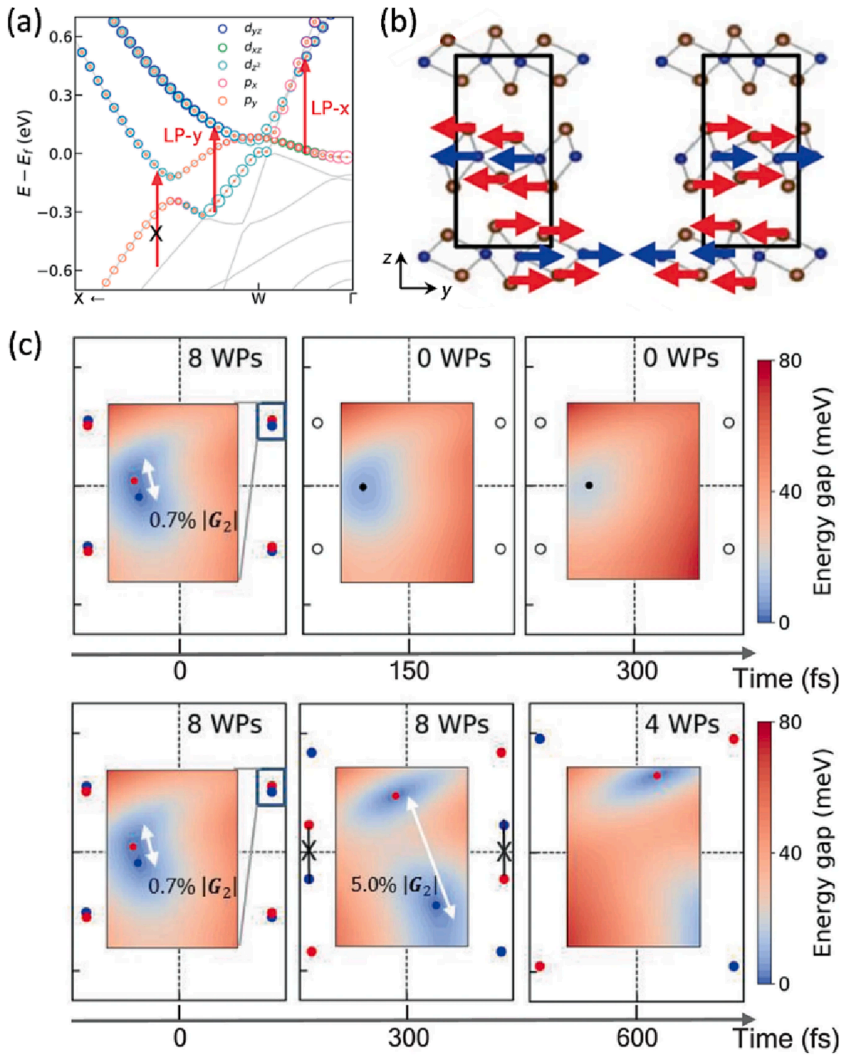

Fig. 8. Transient Weyl fermions from photoexcitation-induced interlayer displacements in the 3D orthorhombic WTe_2 driven by short-duration Gaussian light pulses with the photon energy of 0.6 eV, FWHM of 10 fs, and intensity of 6.5×10^{10} W/cm^2. (a) Electronic band structure of equilibrium WTe_2. On the Weyl cones around W point, electronic states are contributed by W-5d and Te-5p orbitals. Red arrows represent two types of photoexcitation of electrons, induced by the light fields of LP-x and LP-y with the linear polarization along x and y directions, respectively. (b) Illustration of the interlayer displacements induced by LP-x (left panel) and LP-y (right panel) fields. (c) Time evolution of the $\boldsymbol{k}$-space location of the Weyl points driven by LP-x (top panel) and LP-y (bottom panel) light pulses. Adapted from [92]. (For interpretation of the references to colour in this figure legend, the reader is referred to the web version of this article.)

controlled by irradiating short light pulses without time periodicity, in which transient electronic states evolve with time [1–3]. To show the relation between transient and Floquet states, an example on dynamically controlling Weyl fermions is presented here [92].

Without inversion symmetry, the Weyl semimetal of orthorhombic WTe_2 has four pairs of type-II Weyl nodal points at the plane of $k_z = 0$ in the reciprocal BZ. As shown in Fig. 8(a), the electronic states around Weyl point are mainly contributed by W-5d_{yz,xz,z^2} and Te-5$p_{x,y}$ orbitals. As a result, the light field, labeled as LP-x (LP-y), with linear polarization along x (y) direction induces the electron excitation from occupied Te-5p_x and W-5d_{xz} (W-5d_{z^2}) orbitals to empty W-5d_{z^2} (W-5d_{yz}) orbital for the states on the W-Γ (W-X) path. Due to strong electron–phonon couplings in the orthorhombic WTe_2, the photoexcitation of electrons leads to structure modification. With the photoexcitation induced by the LP-x (LP-y) pulse, one layer moves toward $-y$ ($+y$) direction, and the other layer moves toward $+y$ ($-y$) direction [Fig. 8(b)], which diminishes (enlarges) the distance of the pair of Weyl points, as shown in Fig. 8(c). More importantly, the interlayer displacements can become large enough to merge two Weyl points with the opposite (same) topological

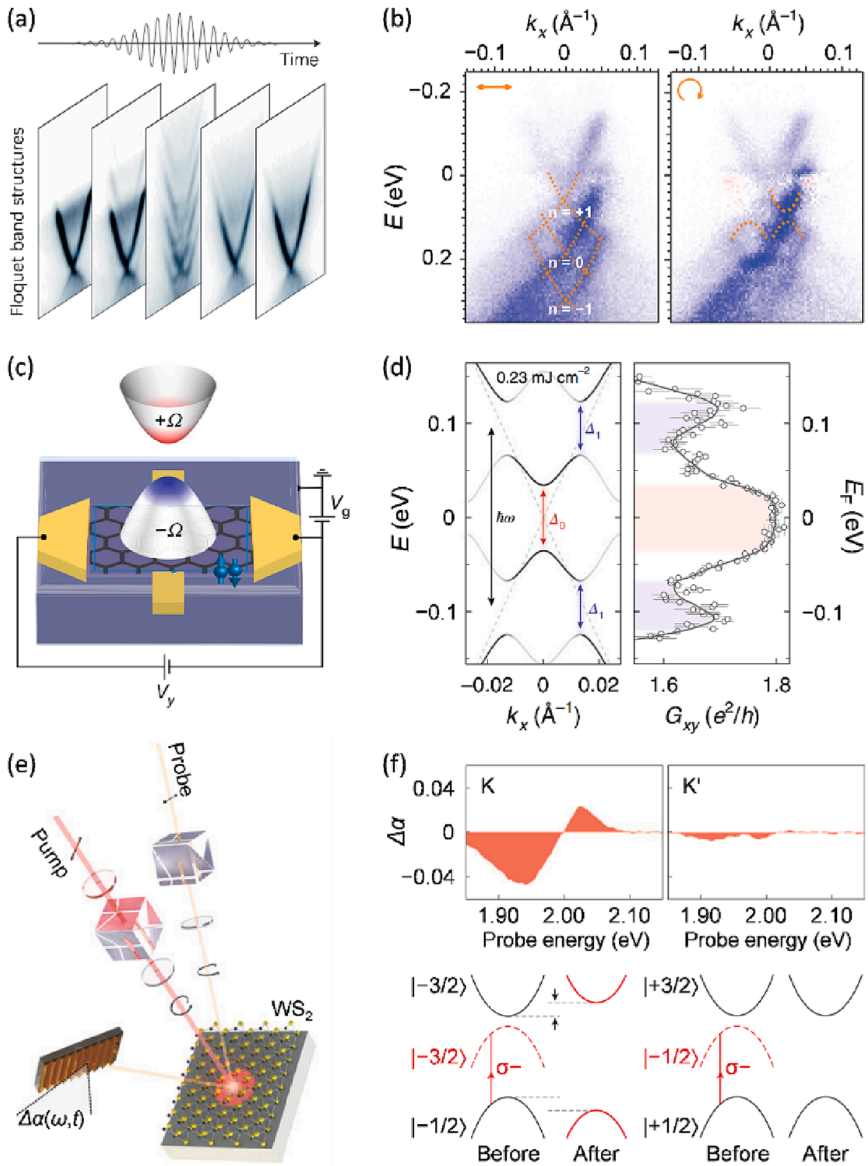

Fig. 9. Experimental observations of light-induced Floquet electronic states. (a,b) Tr-ARPES of Floquet-Dirac states on the surface of light-driven Bi_2Se_3. (a) Evolution of Dirac states with the envelope of a long-duration pump pulse. (b) Floquet-Dirac states under the linearly (left panel) and circularly (right panel) polarized pump pulses without delay time to probe pulses. (c,d) Transport measurement of Floquet anomalous Hall effect in CPL-illuminated graphene. Hall conductance was observed with changing the Fermi energy of driven graphene [right panel of (d)]. Floquet-Dirac bands are simulated with the same light frequency and amplitude to that in experiments [left panel of (d)]. (e,f) Optical absorption of Floquet energy valleys in the WS_2 driven by a CPL with the photon energy just below band gap. The change ($\Delta\alpha$) of absorption spectrum is measured for K and K' valleys under a left-handed (σ^-) CPL [upper panels of (f)]. In sketched Floquet-Bloch bands [lower panels of (f)], magnetic quantum numbers of energy valleys are marked. Adapted from [82–86,221].

charges, shown by the transient state at the time of 300 fs (600 fs). Therefore, the position of Weyl nodal points can be dynamically controlled by illuminating ultrashort light pulses, where the more flexible control of Weyl fermions in the WTe_2 can be found in [92].

This theoretical work was done through using the ab-initio software of TDAP [109]. The illumination of short-duration pulses dynamically engineer transient topological states through light-matter interactions, which does not depend on the required time periodicity of light driving for Floquet engineering. On the other hand, with long-enough-duration light pulses, time periodicity could be approximately reached to create Floquet steady states, where the Floquet states evolve with the envelope of pulses.

5. Experiments on Floquet-Bloch electronic states

So far, various experiments have already demonstrated the light-induced Floquet electronic states with nontrivial band topology, where time periodicity is reached by irradiating long-duration light pulses. As examples, three types of experiments on the Floquet states, which are inspired by theoretical predictions, are presented in this Section, including the measurement of tr-ARPES, electronic transport, and optical absorption for the light-driven crystals of Bi_2Se_3, graphene, and WS_2, respectively [82–86].

Through measuring the tr-ARPES for light-driven Dirac surface states of Bi_2Se_3, the first observation of topological Floquet states was achieved [82,83], in which pump and probe light pulses induce and detect Floquet electronic bands, respectively. As shown in Fig. 9(a), the light-induced Floquet-Dirac bands evolve with the envelope of a pump pulse. Both the original Dirac bands (indexed by $n = 0$), and the photon-dressed Dirac bands (indexed by $n \neq 0$) were observed. In particular, illuminated by a circularly (linearly) polarized pump pulse, the $n = 0$ Dirac cone and its dressed $n = \pm 1$ replicas become gapped (keep gapless); meanwhile, the crossings of $n = 0$ and $n = \pm 1$ Dirac bands give rise to new gapped (gapless) Dirac cones, as shown in Fig. 9(b). Furthermore, another tr-ARPES experiment, also for the light-driven Bi_2Se_3, not only observed Floquet states, but also demonstrated electron scatterings between the light-driven Floquet and Volkov states [84,107,108]. Similarly, the rich Floquet topological bands from theoretical predictions, presented for real materials in Section 3, are very likely to be experimentally confirmed through tr-ARPES measurements.

Anomalous Hall effect from the gapped Floquet-Dirac cones has been shown by measuring the electronic transport in CPL-driven graphene [Fig. 9(c)], which is the first experimental study on transport properties of light-induced Floquet electronic states [85]. As shown in Fig. 9(d), under a CPL with the photon energy 0.19 eV and light intensity 0.23 mJ/cm^{-2}, anomalous Hall conductance plateaus emerge at both the Dirac gap Δ_0 of $n = 0$ bands and the band gaps Δ_1 from avoided crossings of $n = 0$ and dressed $n = \pm 1$ Dirac bands. The conductance plateau at Δ_0 has a width of 60 meV, agreeing with the corresponding gap of 69 meV in simulated Floquet-Dirac bands. This measurement directly confirmed the photovoltaic Hall effect in light-driven graphene as proposed in a milestone paper [27]. Another theoretical paper, using first-principles calculations, explained this experiment in detail, showing that the light-induced Hall current is contributed by both the anomalous topological velocity from Berry curvature and the imbalance of electron population of Floquet-Dirac bands [78]. One can thus expect that the high-temperature Floquet FQHE in a Kagome material, discussed in Section 3.5, can be observed by the similar type of transport measurement in experiments.

As illustrated in Fig. 9(e), by detecting optical absorption of electrons in the TMD material of monolayer WS_2, light-controlled Floquet energy valleys were experimentally demonstrated [86]. Driven by a CPL with left helicity (σ^-), the absorption spectrum α of WS_2 changes as the $\Delta\alpha = \alpha_{\mathrm{driven}} - \alpha_{\mathrm{original}}$ in Fig. 9(f). For K valley, $\Delta\alpha$ is positive (and negative) at the energy higher (and lower) than the original absorption peak at 2.0 eV, showing that absorption peak is shifted to a higher energy. This corresponds to the upward shift of CBM and downward shift of VBM for a larger band gap, as illustrated in Fig. 9(f). In detail, the VBM with a magnetic quantum number $m = -1/2$ absorbs a photon to form the dressed $n = 1$ VBM with $m = -3/2$; the CBM has the same $m = -3/2$ to that of the $n = 1$ VBM, thus they are repulsive with each other due to optical Stark effects, giving rise to the upward-shifted CBM. Similarly, band repulsion between the VBM and $n = -1$ CBM with the same $m = -1/2$ leads to the downward-shifted VBM. In contrast, for driven K' valley, the CBM and $n = 1$ VBM, also the VBM and $n = -1$ CBM, have different values of m, so there is no optical Stark effect, i.e., no band repulsion, which was experimentally demonstrated by the observed $\Delta\alpha \sim 0$. To induce optical Stark effects at K' valley, the CPL with right helicity (σ^+) should be applied to produce the same m of the CBM and $n = 1$ VBM, also of the VBM and $n = -1$ CBM. Moreover, another experiment on optical absorption, also for the Floquet valleys of light-driven WS_2, demonstrated the shifted energy valleys that are originated from Bloch-Siegert effects [88]. With the techniques of transient optical absorption of electrons, the predicted Floquet conversion of bright and dark valley excitons in TMDs, shown in Section 3.4, can also be confirmed by experiments.

In these experiments, the flexible controllability of the topological Floquet states in real crystalline materials signifies a great potential of employing the Floquet-Bloch electronic states to fabricate topological devices. However, in comparison with the already-enormous theoretical proposals, more experiments on the topological Floquet electronic states are expected and desired, which has been laid down in various realistic light-matter coupled systems as predicted by ab-initio computational studies [79–81,90,91,129,134,186], such as that presented in Section 3.

In addition, the Floquet-Bloch states with trivial band topology have been experimentally demonstrated in pump–probe setups, such as the light-driven surface and bulk electronic states of metallic copper and semiconducting BP, respectively. With measurements of time-resolved multiphoton photoemission spectroscopy for Cu(1 1 1) surface, the optically-shifted Shockley and image potential bands, and their photon-dressed replica bands are observed, where the effective mass of the surface electronic bands is modified by time-periodic light illumination [96,97]. With tr-ARPES measurements for 3D BP, a strong band renormalization is discovered near the band edges of energy gaps, which requires the pump light field with the linear polarization along armchair direction, named by pseudospin-selective Floquet engineering [98]. Therefore, Floquet light driving can flexibly engineer both the topologically nontrivial and trivial electronic states, and thus give rise to various intriguing controllable physical phenomena.

6. Summary and perspective

In summary, this work mainly reviews our recent progresses in ab-initio predictions of the topological Floquet electronic states in real crystals under time-periodic light fields. With a Floquet-Wannier modeling scheme, a series of the light-controlled steady electronic structures were discovered, which include the Floquet-Dirac fermions in graphene and BP, the Floquet bright and dark valley excitons in monolayer TMDs, and the Floquet-Chern FBs in a Kagome material. Importantly, these theoretical predictions not only identified the intriguing Floquet states, but also provided the realistic light-material coupled systems for their realization. Complementary to these achievements, the transient Weyl fermions, driven by time-aperiodic ultrashort light pulses, are also presented. In addition, with measuring the tr-ARPES, electronic transport, and optical absorption of Floquet electronic states, three prominent experiments are introduced, showing that the light-induced topological Floquet states can be now realized in current experimental settings. All these studies demonstrate that light illumination is an effective way to engineer topological electronic states in quantum materials.

Besides single-particle states, time-periodic light irradiation can also control many-particle electronic states with strong Coulomb interactions. Through effective toy models, the Floquet magnetization [190,191], Floquet-Mott insulators [192–194], Floquet-Luttinger liquids [195,196], and Floquet states at metal surfaces [107,197,198] have been theoretically proposed. However, there is very few ab-initio predictions of the realistic quantum materials for the novel correlated Floquet electronic states, which stems from the heaviness and inadequate accuracy of the relevant calculations at present. As a new method, the Floquet-Wannier modeling scheme, presented in Section 2.3, can be combined with many-body approaches, e.g., the dynamical mean field theory and the influence matrix method [199–217], to model correlated Floquet states in realistic materials, which is practicable with small computational costs. As a result, by revealing realistic systems for many-particle Floquet states, the current first-principles predictions, only for single-particle Floquet electronic states, will be extended.

Also rooted in light-matter interactions, other two approaches, dubbed cavity and Poincaré engineering, have emerged to control quantum properties of matter. In comparison with Floquet engineering, the cavity engineering has the similar theoretical formulations but completely different physical origins [218–225], where the materials in dark cavities are modified through coupling to virtual photon modes from vacuum fluctuation in quantum electrodynamics. The coupling is tunable by changing cavity configurations, in which strong coupling from enhanced quantum fluctuation, in the cavities with a high quality factor, can be achieved to alter materials properties dramatically, such as the accelerated molecular reactivity [226], controlled magneto-transport of electrons [227], driven exciton polaritons [228], and modulated electron–phonon couplings [229]. Importantly, beyond Floquet materials, the quantum materials in dark cavities, which can be engineered by changing virtual cavity modes, are in the ground state with neither electron excitation nor lattice heating. Thus, the cavity materials engineering, with the similar advantages as Floquet engineering while without their corresponding disadvantages, should be an excellent way to control the ground-state electronic states for achieving the new and ideal topological states with perfect quantization, which will be comprehensively explored in the near future. Besides, inputting real photons in cavities is intriguing to, quantum electrodynamically, engineer nonequilibrium electronic states in materials [221,230].

In contrast with space-homogeneous fields in Floquet engineering, the Poincaré materials engineering employs space-inhomogeneous structured fields with non-uniform profiles of light polarization [231]. With the Stokes parameters of polarization to encompass regions of Poincaré sphere, the symmetries and interactions of quantum materials would be modified by the textured vectorial light fields. The light-matter interactions, different from that for space-uniform fields, can expand the optical Floquet control of fundamental materials properties, such as topological electronic states. As a new and controllable degree of freedom, the spatial profile of light polarization may be combined with tunable time profile, e.g., Floquet time periodicity, of light fields for more intriguing physical phenomena in nonequilibrium states. The structured fields can be currently realizable by using the plasmon polaritons on metal surfaces or interfaces [232], and by shaping the light fields in optical cavities [225].

As an example, plasmonic vortex is a structured light field with antiparallel electric ($\boldsymbol{E}$) and magnetic ($\boldsymbol{H}$) fields at vortex core, which can bring about various applications [231,233–235]. First, by breaking time-reversal symmetry, a vortex core with the pseudoscalar $\boldsymbol{E} \bullet \boldsymbol{H}$ focus can induce a dynamical axion field in illuminated materials, which renders the flexible control of topological magnetoelectric effect in nanometer scale. Second, with a time-periodic evolution of plasmonic vortex, the Poincaré engineering can be combined with Floquet engineering for creating exotic phenomena, such as the manipulation of axion quasiparticles in condensed matter. Third, plasmonic vortex can be applied on quantum materials to control magnetic states via inverse Faraday effect, such as the ultrafast demagnetization or magnetization, which would expand the scope of magnetism control currently by conventional unstructured light fields [236]. Hence, the Poincaré engineering should be a good way to extend the current Floquet engineering for more controllable quantum states of matter. Overall, engineering quantum materials via light-matter interactions is a promising research area with attractive physical phenomena, and their resultant potential applications yet to come in next few years.

Declaration of Competing Interest

The authors declare that they have no known competing financial interests or personal relationships that could have appeared to influence the work reported in this paper.

Acknowledgments

The authors acknowledge financial support from the Ministry of Science and Technology of China (Grant No. 2021YFA1400201), National Natural Science Foundation of China (Grants No. 12025407, No. 11934003, No. 12204338, and No. 12147136), Chinese

Academy of Sciences (Grants No. XDB330301 and No. YSBR047), Guangdong Basic and Applied Basic Research Foundation (Grant No. 2021A1515110466), and China Postdoctoral Science Foundation (Grants No. 2021M700163 and No. 2022T150693).

References

[1] A. de la Torre, D.M. Kennes, M. Claassen, S. Gerber, J.W. McIver, M.A. Sentef, Colloquium: Nonthermal pathways to ultrafast control in quantum materials, Rev. Mod. Phys. 93 (2021), 041002.
[2] J. Lloyd-Hughes, P.M. Oppeneer, T. Pereira dos Santos, A. Schleife, S. Meng, M.A. Sentef, M. Ruggenthaler, A. Rubio, I. Radu, M. Murnane, X. Shi, H. Kapteyn, B. Stadtmüller, K.M. Dani, F.H. da Jornada, E. Prinz, M. Aeschlimann, R.L. Milot, M. Burdanova, J. Boland, T. Cocker, F. Hegmann, The 2021 ultrafast spectroscopic probes of condensed matter roadmap, J. Phys. Condens. Matter 33 (2021), 353001.
[3] A.S. Disa, T.F. Nova, A. Cavalleri, Engineering crystal structures with light, Nat. Phys. 17 (2021) 1087.
[4] T. Oka, S. Kitamura, Floquet engineering of quantum materials, Annu. Rev. Condens. Matter Phys. 10 (2019) 387.
[5] M.S. Rudner, N.H. Lindner, Band structure engineering and non-equilibrium dynamics in Floquet topological insulators, Nat. Rev. Phys. 2 (2020) 229.
[6] M.G. Floquet, Sur les équations différentielles linéaires à coefficients périodiques, Ann. Ec. Norm. Suppl. 12 (1883) 47.
[7] J.H. Shirley, Solution of the Schrödinger equation with a Hamiltonian periodic in time, Phys. Rev. 138 (1965) B979.
[8] H. Sambe, Steady states and quasienergies of a quantum-mechanical system in an oscillating field, Phys. Rev. A 7 (1973) 2203.
[9] K.F. Milfeld, R.E. Wyatt, Study, extension, and application of Floquet theory for quantum molecular systems in an oscillating field, Phys. Rev. A 27 (1983) 72.
[10] M. Bukov, L. D'Alessio, A. Polkovnikov, Universal high-frequency behavior of periodically driven systems: from dynamical stabilization to Floquet engineering, Adv. Phys. 64 (2015) 139.
[11] B.-Q. Wang, H. Wu, J.-H. An, Engineering exotic second-order topological semimetals by periodic driving, Phys. Rev. B 104 (2021), 205117.
[12] B.M. Fregoso, Y.H. Wang, N. Gedik, V. Galitski, Driven electronic states at the surface of a topological insulator, Phys. Rev. B 88 (2013), 155129.
[13] Y.T. Katan, D. Podolsky, Modulated Floquet topological insulators, Phys. Rev. Lett. 110 (2013), 016802.
[14] Y. Tenenbaum Katan, D. Podolsky, Generation and manipulation of localized modes in Floquet topological insulators, Phys. Rev. B 88 (2013), 224106.
[15] J.I. Inoue, A. Tanaka, Photoinduced transition between conventional and topological insulators in two-dimensional electronic systems, Phys. Rev. Lett. 105 (2010), 017401.
[16] M. Tahir, Q.Y. Zhang, U. Schwingenschlogl, Floquet edge states in germanene nanoribbons, Sci. Rep. 6 (2016) 31821.
[17] M. Hasan, D. Yudin, I. Iorsh, O. Eriksson, I. Shelykh, Topological edge-state engineering with high-frequency electromagnetic radiation, Phys. Rev. B 96 (2017), 205127.
[18] B. Dora, J. Cayssol, F. Simon, R. Moessner, Optically engineering the topological properties of a spin Hall insulator, Phys. Rev. Lett. 108 (2012), 056602.
[19] H. Dehghani, A. Mitra, Occupation probabilities and current densities of bulk and edge states of a Floquet topological insulator, Phys. Rev. B 93 (2016), 205437.
[20] T. Kitagawa, T. Oka, A. Brataas, L. Fu, E. Demler, Transport properties of nonequilibrium systems under the application of light: Photoinduced quantum Hall insulators without Landau levels, Phys. Rev. B 84 (2011), 235108.
[21] Z. Zhou, I.I. Satija, E. Zhao, Floquet edge states in a harmonically driven integer quantum Hall system, Phys. Rev. B 90 (2014), 205108.
[22] H.L. Calvo, L.E.F. Foa Torres, P.M. Perez-Piskunow, C.A. Balseiro, G. Usaj, Floquet interface states in illuminated three-dimensional topological insulators, Phys. Rev. B 91 (2015), 241404.
[23] M.A. Sentef, M. Claassen, A.F. Kemper, B. Moritz, T. Oka, J.K. Freericks, T.P. Devereaux, Theory of Floquet band formation and local pseudospin textures in pump-probe photoemission of graphene, Nat. Commun. 6 (2015) 7047.
[24] K. Kristinsson, O.V. Kibis, S. Morina, I.A. Shelykh, Control of electronic transport in graphene by electromagnetic dressing, Sci. Rep. 6 (2016) 20082.
[25] M. Puviani, F. Manghi, A. Bertoni, Dynamics and control of edge states in laser-driven graphene nanoribbons, Phys. Rev. B 95 (2017), 235430.
[26] M. Yang, Z.-J. Cai, R.-Q. Wang, Y.-K. Bai, Topologically trivial and nontrivial edge bands in graphene induced by irradiation, Phys. Lett. A 380 (2016) 2836.
[27] T. Oka, H. Aoki, Photovoltaic Hall effect in graphene, Phys. Rev. B 79 (2009) 081406(R).
[28] P.M. Perez-Piskunow, G. Usaj, C.A. Balseiro, L.E.F. Foa Torres, Floquet chiral edge states in graphene, Phys. Rev. B 89 (2014), 121401.
[29] G. Usaj, P.M. Perez-Piskunow, L.E.F. Foa Torres, C.A. Balseiro, Irradiated graphene as a tunable Floquet topological insulator, Phys. Rev. B 90 (2014), 115423.
[30] N.H. Lindner, G. Refael, V. Galitski, Floquet topological insulator in semiconductor quantum wells, Nat. Phys. 7 (2011) 490.
[31] J. Cayssol, B. Dóra, F. Simon, R. Moessner, Floquet topological insulators, Phys. Status Solidi RRL 7 (2013) 101.
[32] N.H. Lindner, D.L. Bergman, G. Refael, V. Galitski, Topological Floquet spectrum in three dimensions via a two-photon resonance, Phys. Rev. B 87 (2013), 235131.
[33] M. Lababidi, I.I. Satija, E. Zhao, Counter-propagating edge modes and topological phases of a kicked quantum Hall system, Phys. Rev. Lett. 112 (2014), 026805.
[34] T. Morimoto, N. Nagaosa, Topological nature of nonlinear optical effects in solids, Sci. Adv. 2 (2016) e1501524.
[35] P. Titum, N.H. Lindner, G. Refael, Disorder-induced transitions in resonantly driven Floquet topological insulators, Phys. Rev. B 96 (2017), 054207.
[36] C. Dutreix, E.A. Stepanov, M.I. Katsnelson, Laser-induced topological transitions in phosphorene with inversion symmetry, Phys. Rev. B 93 (2016), 241404.
[37] A. Farrell, T. Pereg-Barnea, Edge-state transport in Floquet topological insulators, Phys. Rev. B 93 (2016), 045121.
[38] L. D'Alessio, M. Rigol, Dynamical preparation of Floquet Chern insulators, Nat. Commun. 6 (2015) 8336.
[39] T. Mishra, A. Pallaprolu, T.G. Sarkar, J.N. Bandyopadhyay, Floquet topological phase transitions in a kicked Haldane-Chern insulator, Phys. Rev. B 97 (2017), 085405.
[40] L.C. Wang, X.P. Li, C.F. Li, Effect of periodic kicking on Chern insulators, Phys. Rev. B 95 (2017), 104308.
[41] A.G. Grushin, A. Gomez-Leon, T. Neupert, Floquet fractional Chern insulators, Phys. Rev. Lett. 112 (2014), 156801.
[42] E. Anisimovas, G. Žlabys, B.M. Anderson, G. Juzeliūnas, A. Eckardt, Role of real-space micromotion for bosonic and fermionic Floquet fractional Chern insulators, Phys. Rev. B 91 (2015), 245135.
[43] A. Ghazaryan, T. Graß, M.J. Gullans, P. Ghaemi, M. Hafezi, Light-induced fractional quantum hall phases in graphene, Phys. Rev. Lett. 119 (2017), 247403.
[44] C.H. Lee, W.W. Ho, B. Yang, J. Gong, Z. Papić, Floquet mechanism for non-abelian fractional quantum hall states, Phys. Rev. Lett. 121 (2018), 237401.
[45] S. Li, C.-C. Liu, Y. Yao, Floquet high Chern insulators in periodically driven chirally stacked multilayer graphene, New J. Phys. 20 (2018), 033025.
[46] A. Kundu, H.A. Fertig, B. Seradjeh, Floquet-engineered valleytronics in dirac systems, Phys. Rev. Lett. 116 (2016), 016802.
[47] M. Luo, Floquet states of valley-polarized metal with one-way spin or charge transport in zigzag nanoribbons, Phys. Rev. B 99 (2019), 075406.
[48] R. Wang, B. Wang, R. Shen, L. Sheng, D.Y. Xing, Floquet Weyl semimetal induced by off-resonant light, EPL (Europhysics Letters) 105 (2014) 17004.
[49] C.K. Chan, P.A. Lee, K.S. Burch, J.H. Han, Y. Ran, When chiral photons meet chiral fermions: photoinduced anomalous hall effects in weyl semimetals, Phys. Rev. Lett. 116 (2016), 026805.
[50] C.-K. Chan, Y.-T. Oh, J.H. Han, P.A. Lee, Type-II Weyl cone transitions in driven semimetals, Phys. Rev. B 94 (2016) 121106(R).
[51] Z. Yan, Z. Wang, Tunable Weyl Points in Periodically Driven Nodal Line Semimetals, Phys. Rev. Lett. 117 (2016), 087402.
[52] S.V. Syzranov, Y.I. Rodionov, K.I. Kugel, F. Nori, Strongly anisotropic Dirac quasiparticles in irradiated graphene, Phys. Rev. B 88 (2013) 241112(R).
[53] J.-Y. Zou, B.-G. Liu, Floquet Weyl fermions in three-dimensional stacked graphene systems irradiated by circularly polarized light, Phys. Rev. B 93 (2016), 205435.
[54] Z. Yan, Z. Wang, Floquet multi-Weyl points in crossing-nodal-line semimetals, Phys. Rev. B 96 (2017) 041206(R).
[55] R. Chen, B. Zhou, D.-H. Xu, Floquet Weyl semimetals in light-irradiated type-II and hybrid line-node semimetals, Phys. Rev. B 97 (2018), 155152.
[56] S. Koghee, L.-K. Lim, M.O. Goerbig, C.M. Smith, Merging and alignment of Dirac points in a shaken honeycomb optical lattice, Phys. Rev. A 85 (2012), 023637.
[57] P. Delplace, Á. Gómez-León, G. Platero, Merging of Dirac points and Floquet topological transitions in ac-driven graphene, Phys. Rev. B 88 (2013), 245422.

[58] M. Ezawa, Photoinduced topological phase transition and a single Dirac-cone state in silicene, Phys. Rev. Lett. 110 (2013), 026603.
[59] Q. Chen, L. Du, G.A. Fiete, Floquet band structure of a semi-Dirac system, Phys. Rev. B 97 (2018), 035422.
[60] M. Ezawa, Chiral anomaly enhancement and photoirradiation effects in multiband touching fermion systems, Phys. Rev. B 95 (2017), 205201.
[61] R. Jaiswal, A. Narayan, Floquet engineering of multifold fermions, Phys. Rev. B 102 (2020), 245416.
[62] L. Li, C.H. Lee, J. Gong, Realistic Floquet semimetal with exotic topological linkages between arbitrarily many nodal loops, Phys. Rev. Lett. 121 (2018), 036401.
[63] M.S. Rudner, N.H. Lindner, E. Berg, M. Levin, Anomalous edge states and the bulk-edge correspondence for periodically driven two-dimensional systems, Phys. Rev. X 3 (2013), 031005.
[64] T. Kitagawa, E. Berg, M. Rudner, E. Demler, Topological characterization of periodically driven quantum systems, Phys. Rev. B 82 (2010), 235114.
[65] A. Gomez-Leon, G. Platero, Floquet-Bloch theory and topology in periodically driven lattices, Phys. Rev. Lett. 110 (2013), 200403.
[66] D. Carpentier, P. Delplace, M. Fruchart, K. Gawedzki, Topological index for periodically driven time-reversal invariant 2D systems, Phys. Rev. Lett. 114 (2015), 106806.
[67] S.T. Pi, S. Savrasov, Polarization induced Z_2 and Chern topological phases in a periodically driving field, Sci. Rep. 6 (2016) 22993.
[68] B. Höckendorf, A. Alvermann, H. Fehske, Topological invariants for Floquet-Bloch systems with chiral, time-reversal, or particle-hole symmetry, Phys. Rev. B 97 (2018), 045140.
[69] M. Rodriguez-Vega, B. Seradjeh, Universal fluctuations of floquet topological invariants at low frequencies, Phys. Rev. Lett. 121 (2017), 036402.
[70] T. Iadecola, T.H. Hsieh, Floquet supersymmetry, Phys. Rev. Lett. 120 (2017), 210603.
[71] T. Morimoto, H.C. Po, A. Vishwanath, Floquet topological phases protected by time glide symmetry, Phys. Rev. B 95 (2017), 195155.
[72] I.D. Potirniche, A.C. Potter, M. Schleier-Smith, A. Vishwanath, N.Y. Yao, Floquet symmetry-protected topological phases in cold-atom systems, Phys. Rev. Lett. 119 (2017), 123601.
[73] A.C. Potter, T. Morimoto, Dynamically enriched topological orders in driven two-dimensional systems, Phys. Rev. B 95 (2017), 155126.
[74] R. Roy, F. Harper, Floquet topological phases with symmetry in all dimensions, Phys. Rev. B 95 (2017), 195128.
[75] R. Roy, F. Harper, Periodic table for Floquet topological insulators, Phys. Rev. B 96 (2017), 155118.
[76] S. Yao, Z. Yan, Z. Wang, Topological invariants of Floquet systems: General formulation, special properties, and Floquet topological defects, Phys. Rev. B 96 (2017), 195303.
[77] W. Zhu, Y.D. Chong, J. Gong, Symmetry analysis of anomalous Floquet topological phases, Phys. Rev. B 104 (2021) L020302.
[78] S.A. Sato, J.W. McIver, M. Nuske, P. Tang, G. Jotzu, B. Schulte, H. Hübener, U. De Giovannini, L. Mathey, M.A. Sentef, A. Cavalleri, A. Rubio, Microscopic theory for the light-induced anomalous Hall effect in graphene, Phys. Rev. B 99 (2019), 214302.
[79] Z.F. Wang, Z. Liu, J. Yang, F. Liu, Light-induced type-II band inversion and quantum anomalous hall state in monolayer FeSe, Phys. Rev. Lett. 120 (2018), 156406.
[80] M. Claassen, C. Jia, B. Moritz, T.P. Devereaux, All-optical materials design of chiral edge modes in transition-metal dichalcogenides, Nat. Commun. 7 (2016) 13074.
[81] U. De Giovannini, H. Hubener, A. Rubio, Monitoring electron-photon dressing in WSe_2, Nano Lett. 16 (2016) 7993.
[82] Y.H. Wang, H. Steinberg, P. Jarillo-Herrero, N. Gedik, Observation of Floquet-Bloch states on the surface of a topological insulator, Science 342 (2013) 453.
[83] D.N. Basov, R.D. Averitt, D. Hsieh, Towards properties on demand in quantum materials, Nat. Mater. 16 (2017) 1077.
[84] F. Mahmood, C.-K. Chan, Z. Alpichshev, D. Gardner, Y. Lee, P.A. Lee, N. Gedik, Selective scattering between Floquet-Bloch and Volkov states in a topological insulator, Nat. Phys. 12 (2016) 306.
[85] J.W. McIver, B. Schulte, F.U. Stein, T. Matsuyama, G. Jotzu, G. Meier, A. Cavalleri, Light-induced anomalous Hall effect in graphene, Nat. Phys. 16 (2020) 38.
[86] E.J. Sie, J.W. McIver, Y.H. Lee, L. Fu, J. Kong, N. Gedik, Valley-selective optical Stark effect in monolayer WS_2, Nat. Mater. 14 (2015) 290.
[87] T. LaMountain, H. Bergeron, I. Balla, T.K. Stanev, M.C. Hersam, N.P. Stern, Valley-selective optical Stark effect probed by Kerr rotation, Phys. Rev. B 97 (2018), 045307.
[88] E.J. Sie, C.H. Lui, Y.-H. Lee, L. Fu, J. Kong, N. Gedik, Large, valley-exclusive Bloch-Siegert shift in monolayer WS_2, Science 355 (2017) 1066.
[89] S. Aeschlimann, S.A. Sato, R. Krause, M. Chavez-Cervantes, U. De Giovannini, H. Hubener, S. Forti, C. Coletti, K. Hanff, K. Rossnagel, A. Rubio, I. Gierz, Survival of Floquet-Bloch states in the presence of scattering, Nano Lett. 21 (2021) 5028.
[90] H. Hubener, M.A. Sentef, U. De Giovannini, A.F. Kemper, A. Rubio, Creating stable Floquet-Weyl semimetals by laser-driving of 3D Dirac materials, Nat. Commun. 8 (2017) 13940.
[91] H. Liu, J.-T. Sun, C. Cheng, F. Liu, S. Meng, Photoinduced nonequilibrium topological states in strained black phosphorus, Phys. Rev. Lett. 120 (2018), 237403.
[92] M.X. Guan, E. Wang, P.W. You, J.T. Sun, S. Meng, Manipulating Weyl quasiparticles by orbital-selective photoexcitation in WTe_2, Nat. Commun. 12 (2021) 1885.
[93] G.E. Topp, N. Tancogne-Dejean, A.F. Kemper, A. Rubio, M.A. Sentef, All-optical nonequilibrium pathway to stabilising magnetic Weyl semimetals in pyrochlore iridates, Nat. Commun. 9 (2018) 4452.
[94] D.M. Kennes, E.Y. Wilner, D.R. Reichman, A.J. Millis, Transient superconductivity from electronic squeezing of optically pumped phonons, Nat. Phys. 13 (2017) 479.
[95] R. Mankowsky, A. Subedi, M. Först, S.O. Mariager, M. Chollet, H.T. Lemke, J.S. Robinson, J.M. Glownia, M.P. Minitti, A. Frano, M. Fechner, N.A. Spaldin, T. Loew, B. Keimer, A. Georges, A. Cavalleri, Nonlinear lattice dynamics as a basis for enhanced superconductivity in $YBa_2Cu_3O_{6.5}$, Nature 516 (2014) 71.
[96] M. Reutzel, A. Li, Z. Wang, H. Petek, Coherent multidimensional photoelectron spectroscopy of ultrafast quasiparticle dressing by light, Nat. Commun. 11 (2020) 2230.
[97] M. Reutzel, A. Li, H. Petek, Coherent two-dimensional multiphoton photoelectron spectroscopy of metal surfaces, Phys. Rev. X 9 (2019), 011044.
[98] S. Zhou, C. Bao, B. Fan, H. Zhou, Q. Gao, H. Zhong, T. Lin, H. Liu, P. Yu, P. Tang, S. Meng, W. Duan, S. Zhou, Pseudospin-selective Floquet band engineering in black phosphorus, Nature 614 (2023) 75.
[99] T. Čadež, R. Mondaini, P.D. Sacramento, Edge and bulk localization of Floquet topological superconductors, Phys. Rev. B 99 (2019), 014301.
[100] S.H. Autler, C.H. Townes, Stark effect in rapidly varying fields, Phys. Rev. 100 (1955) 703.
[101] J. Reimann, S. Schlauderer, C.P. Schmid, F. Langer, S. Baierl, K.A. Kokh, O.E. Tereshchenko, A. Kimura, C. Lange, J. Gudde, U. Hofer, R. Huber, Subcycle observation of lightwave-driven Dirac currents in a topological surface band, Nature 562 (2018) 396.
[102] S. Blanes, F. Casas, J.A. Oteo, J. Ros, The Magnus expansion and some of its applications, Phys. Rep. 470 (2009) 151.
[103] G. Kresse, J. Furthmuller, Efficient iterative schemes for ab initio total-energy calculations using a plane-wave basis set, Phys. Rev. B 54 (1996) 11169.
[104] A.A. Mostofi, J.R. Yates, Y.S. Lee, I. Souza, D. Vanderbilt, N. Marzari, wannier90: A tool for obtaining maximally-localised Wannier functions, Comput. Phys. Commun. 178 (2008) 685.
[105] J.K. Freericks, H.R. Krishnamurthy, T. Pruschke, Theoretical description of time-resolved photoemission spectroscopy: application to pump-probe experiments, Phys. Rev. Lett. 102 (2009), 136401.
[106] A. Farrell, A. Arsenault, T. Pereg-Barnea, Dirac cones, Floquet side bands, and theory of time-resolved angle-resolved photoemission, Phys. Rev. B 94 (2016), 155304.
[107] B. Gumhalter, D. Novko, H. Petek, Electron emission from plasmonically induced Floquet bands at metal surfaces, Phys. Rev. B 106 (2022), 035422.
[108] S.T. Park, Interference in Floquet-Volkov transitions, Phys. Rev. A 90 (2014), 013420.
[109] S. Meng, E. Kaxiras, Real-time, local basis-set implementation of time-dependent density functional theory for excited state dynamics simulations, J. Chem. Phys. 129 (2008), 054110.
[110] N. Tancogne-Dejean, M.J.T. Oliveira, X. Andrade, H. Appel, C.H. Borca, G. Le Breton, F. Buchholz, A. Castro, S. Corni, A.A. Correa, U. De Giovannini, A. Delgado, F.G. Eich, J. Flick, G. Gil, A. Gomez, N. Helbig, H. Hubener, R. Jestadt, J. Jornet-Somoza, A.H. Larsen, I.V. Lebedeva, M. Luders, M.A.L. Marques, S.

T. Ohlmann, S. Pipolo, M. Rampp, C.A. Rozzi, D.A. Strubbe, S.A. Sato, C. Schafer, I. Theophilou, A. Welden, A. Rubio, Octopus, a computational framework for exploring light-driven phenomena and quantum dynamics in extended and finite systems, J. Chem. Phys. 152 (2020), 124119.
[111] X. Wang, A.M. Jones, K.L. Seyler, V. Tran, Y. Jia, H. Zhao, H. Wang, L. Yang, X. Xu, F. Xia, Highly anisotropic and robust excitons in monolayer black phosphorus, Nat. Nanotech. 10 (2015) 517.
[112] F. Xia, H. Wang, Y. Jia, Rediscovering black phosphorus as an anisotropic layered material for optoelectronics and electronics, Nat. Commun. 5 (2014) 4458.
[113] X. Ling, H. Wang, S.X. Huang, F.N. Xia, M.S. Dresselhaus, The renaissance of black phosphorus, Proc. Natl. Acad. Sci. U. S. A. 112 (2015) 4523.
[114] V. Tran, R. Soklaski, Y.F. Liang, L. Yang, Layer-controlled band gap and anisotropic excitons in few-layer black phosphorus, Phys. Rev. B 89 (2014), 235319.
[115] Z. Luo, J. Maassen, Y. Deng, Y. Du, R.P. Garrelts, M.S. Lundstrom, P.D. Ye, X. Xu, Anisotropic in-plane thermal conductivity observed in few-layer black phosphorus, Nat. Commun. 6 (2015) 8572.
[116] G. Zhang, S. Huang, A. Chaves, C. Song, V.O. Ozcelik, T. Low, H. Yan, Infrared fingerprints of few-layer black phosphorus, Nat. Commun. 8 (2017) 14071.
[117] J. Qiao, X. Kong, Z.-X. Hu, F. Yang, W. Ji, High-mobility transport anisotropy and linear dichroism in few-layer black phosphorus, Nat. Commun. 5 (2014) 4475.
[118] L. Li, Y. Yu, G.J. Ye, Q. Ge, X. Ou, H. Wu, D. Feng, X.H. Chen, Y. Zhang, Black phosphorus field-effect transistors, *Nat. Nanotech.* 9 (2014) 372.
[119] J. Kim, S.S. Baik, S.H. Ryu, Y. Sohn, S. Park, B.G. Park, J. Denlinger, Y. Yi, H.J. Choi, K.S. Kim, Observation of tunable band gap and anisotropic Dirac semimetal state in black phosphorus, Science 349 (2015) 723.
[120] B. Deng, V. Tran, Y. Xie, H. Jiang, C. Li, Q. Guo, X. Wang, H. Tian, S.J. Koester, H. Wang, J.J. Cha, Q. Xia, L. Yang, F. Xia, Efficient electrical control of thin-film black phosphorus bandgap, Nat. Commun. 8 (2017) 14474.
[121] J. Kim, S.S. Baik, S.W. Jung, Y. Sohn, S.H. Ryu, H.J. Choi, B.-J. Yang, K.S. Kim, Two-dimensional dirac fermions protected by space-time inversion symmetry in black phosphorus, Phys. Rev. Lett. 119 (2017), 226801.
[122] J. Zhao, R. Yu, H. Weng, Z. Fang, Topological node-line semimetal in compressed black phosphorus, Phys. Rev. B 94 (2016), 195104.
[123] Z.J. Xiang, G.J. Ye, C. Shang, B. Lei, N.Z. Wang, K.S. Yang, D.Y. Liu, F.B. Meng, X.G. Luo, L.J. Zou, Z. Sun, Y. Zhang, X.H. Chen, Pressure-induced electronic transition in black phosphorus, Phys. Rev. Lett. 115 (2015), 186403.
[124] C.-H. Li, Y.-J. Long, L.-X. Zhao, L. Shan, Z.-A. Ren, J.-Z. Zhao, H.-M. Weng, X. Dai, Z. Fang, C. Ren, G.-F. Chen, Pressure-induced topological phase transitions and strongly anisotropic magnetoresistance in bulk black phosphorus, Phys. Rev. B 95 (2017), 125417.
[125] Y. Wang, E. Liu, H. Liu, Y. Pan, L. Zhang, J. Zeng, Y. Fu, M. Wang, K. Xu, Z. Huang, Z. Wang, H.Z. Lu, D. Xing, B. Wang, X. Wan, F. Miao, Gate-tunable negative longitudinal magnetoresistance in the predicted type-II Weyl semimetal WTe_2, Nat. Commun. 7 (2016) 13142.
[126] D. Chen, L.X. Zhao, J.B. He, H. Liang, S. Zhang, C.H. Li, L. Shan, S.C. Wang, Z.A. Ren, C. Ren, G.F. Chen, Magnetotransport properties of the type-II Weyl semimetal candidate Ta_3S_2, Phys. Rev. B 94 (2016), 174411.
[127] F.C. Chen, H.Y. Lv, X. Luo, W.J. Lu, Q.L. Pei, G.T. Lin, Y.Y. Han, X.B. Zhu, W.H. Song, Y.P. Sun, Extremely large magnetoresistance in the type-II Weyl semimetal MoTe2, Phys. Rev. B 94 (2016), 235154.
[128] Z.M. Yu, Y. Yao, S.A. Yang, Predicted unusual magnetoresponse in type-II weyl semimetals, Phys. Rev. Lett. 117 (2016), 077202.
[129] H. Liu, J.-T. Sun, C. Song, H. Huang, F. Liu, S. Meng, Fermionic analogue of high temperature hawking radiation in black phosphorus, Chin. Phys. Lett. 37 (2020), 067101.
[130] K.S. Novoselov, A.K. Geim, S.V. Morozov, D. Jiang, Y. Zhang, S.V. Dubonos, I.V. Grigorieva, A.A. Firsov, Electric field effect in atomically thin carbon films, Science 306 (2004) 666.
[131] A.H. Castro Neto, F. Guinea, N.M.R. Peres, K.S. Novoselov, A.K. Geim, The electronic properties of graphene, Rev. Mod. Phys. 81 (2009) 109.
[132] Y. Cao, V. Fatemi, S. Fang, K. Watanabe, T. Taniguchi, E. Kaxiras, P. Jarillo-Herrero, Unconventional superconductivity in magic-angle graphene superlattices, Nature 556 (2018) 43.
[133] F.D. Haldane, Model for a quantum Hall effect without Landau levels: Condensed-matter realization of the "parity anomaly", Phys. Rev. Lett. 61 (1988) 2015.
[134] H. Liu, J.-T. Sun, S. Meng, Engineering Dirac states in graphene: coexisting type-I and type-II floquet-dirac fermions, Phys. Rev. B 99 (2019), 075121.
[135] T.E. O'Brien, M. Diez, C.W.J. Beenakker, Magnetic breakdown and Klein tunneling in a type-II weyl semimetal, Phys. Rev. Lett. 116 (2016), 236401.
[136] G. Liu, G. Wang, Y. Zhu, H. Zhang, G. Zhang, X. Wang, Y. Zhou, W. Zhang, H. Liu, L. Zhao, J. Meng, X. Dong, C. Chen, Z. Xu, X.J. Zhou, Development of a vacuum ultraviolet laser-based angle-resolved photoemission system with a superhigh energy resolution better than 1meV, Rev. Sci. Instru. 79 (2008), 023105.
[137] G.E. Volovik, K. Zhang, Lifshitz transitions, type-II dirac and weyl fermions, event horizon and all that, J. Low Temp. Phys. 189 (2017) 276.
[138] S. Guan, Z.-M. Yu, Y. Liu, G.-B. Liu, L. Dong, Y. Lu, Y. Yao, S.A. Yang, Artificial gravity field, astrophysical analogues, and topological phase transitions in strained topological semimetals, npj Quantum Mater. 2 (2017) 23.
[139] H. Huang, K.-H. Jin, F. Liu, Black-hole horizon in the Dirac semimetal $Zn_2In_2S_5$, Phys. Rev. B 98 (2018) 121110(R).
[140] A. Westström, T. Ojanen, Designer curved-space geometry for relativistic fermions in weyl metamaterials, Phys. Rev. X 7 (2017), 041026.
[141] W.G. Unruh, Experimental black-hole evaporation? Phys. Rev. Lett. 46 (1981) 1351.
[142] W.G. Unruh, Sonic analogue of black holes and the effects of high frequencies on black hole evaporation, Phys. Rev. D 51 (1995) 2827.
[143] L.J. Garay, J.R. Anglin, J.I. Cirac, P. Zoller, Sonic analog of gravitational black holes in Bose-Einstein condensates, Phys. Rev. Lett. 85 (2000) 4643.
[144] O. Lahav, A. Itah, A. Blumkin, C. Gordon, S. Rinott, A. Zayats, J. Steinhauer, Realization of a sonic black hole analog in a Bose-Einstein condensate, Phys. Rev. Lett. 105 (2010), 240401.
[145] L.J. Garay, J.R. Anglin, J.I. Cirac, P. Zoller, Sonic black holes in dilute Bose-Einstein condensates, Phys. Rev. A 63 (2001), 023611.
[146] J. Steinhauer, Observation of quantum Hawking radiation and its entanglement in an analogue black hole, Nat. Phys. 12 (2016) 959.
[147] B. Horstmann, B. Reznik, S. Fagnocchi, J.I. Cirac, Hawking radiation from an acoustic black hole on an ion ring, Phys. Rev. Lett. 104 (2010), 250403.
[148] S. Giovanazzi, Hawking radiation in sonic black holes, Phys. Rev. Lett. 94 (2005), 061302.
[149] U. Leonhardt, P. Piwnicki, Relativistic effects of light in moving media with extremely low group velocity, Phys. Rev. Lett. 84 (2000) 822.
[150] U. Leonhardt, A laboratory analogue of the event horizon using slow light in an atomic medium, Nature 415 (2002) 406.
[151] R. Schutzhold, W.G. Unruh, Hawking radiation in an electromagnetic waveguide? Phys. Rev. Lett. 95 (2005), 031301.
[152] T.G. Philbin, C. Kuklewicz, S. Robertson, S. Hill, F. Konig, U. Leonhardt, Fiber-optical analog of the event horizon, Science 319 (2008) 1367.
[153] F. Belgiorno, S.L. Cacciatori, M. Clerici, V. Gorini, G. Ortenzi, L. Rizzi, E. Rubino, V.G. Sala, D. Faccio, Hawking radiation from ultrashort laser pulse filaments, Phys. Rev. Lett. 105 (2010), 203901.
[154] R. Schutzhold, W.G. Unruh, Comment on "Hawking radiation from ultrashort laser pulse filaments", Phys. Rev. Lett. 107 (2011), 149401.
[155] M. Elazar, V. Fleurov, S. Bar-Ad, All-optical event horizon in an optical analog of a Laval nozzle, Phys. Rev. A 86 (2012), 063821.
[156] S. Liberati, A. Prain, M. Visser, Quantum vacuum radiation in optical glass, Phys. Rev. D 85 (2012), 084014.
[157] W.G. Unruh, R. Schützhold, On slow light as a black hole analogue, Phys. Rev. D 68 (2003), 024008.
[158] W.G. Unruh, R. Schützhold, Hawking radiation from "phase horizons" in laser filaments? Phys. Rev. D 86 (2012), 064006.
[159] J. Kim, S.S. Baik, S.W. Jung, Y. Sohn, S.H. Ryu, H.J. Choi, B.-J. Yang, K.S. Kim, Two-dimensional dirac fermions protected by space-time inversion symmetry in black phosphorus, Phys. Rev. Lett. 119 (2017), 226801.
[160] A. Roberts, D. Cormode, C. Reynolds, T. Newhouse-Illige, B.J. LeRoy, A.S. Sandhu, Response of graphene to femtosecond high-intensity laser irradiation, Appl. Phys. Lett. 99 (2011), 051912.
[161] W.-H. Dong, D.-L. Bao, J.-T. Sun, F. Liu, S. Du, Manipulation of dirac fermions in nanochain-structured graphene, Chin. Phys. Lett. 38 (2021), 097101.
[162] X. Shao, L. Sun, X. Ma, X. Feng, H. Gao, C. Ding, M. Zhao, Multiple Dirac cones and Lifshitz transition in a two-dimensional Cairo lattice as a Hawking evaporation analogue, J. Phys. Condens. Matter 33 (2021), 365001.
[163] M. Milicevic, G. Montambaux, T. Ozawa, O. Jamadi, B. Real, I. Sagnes, A. Lemaitre, L. Le Gratiet, A. Harouri, J. Bloch, A. Amo, Type-III and tilted dirac cones emerging from flat bands in photonic orbital graphene, Phys. Rev. X 9 (2019), 031010.
[164] D. Xiao, G.B. Liu, W. Feng, X. Xu, W. Yao, Coupled spin and valley physics in monolayers of MoS2 and other group-VI dichalcogenides, Phys. Rev. Lett. 108 (2012), 196802.

[165] J.R. Schaibley, H. Yu, G. Clark, P. Rivera, J.S. Ross, K.L. Seyler, W. Yao, X. Xu, Valleytronics in 2D materials, Nat. Rev. Mater. 1 (2016) 16055.
[166] H. Yu, X. Cui, X. Xu, W. Yao, Valley excitons in two-dimensional semiconductors, Natl. Sci. Rev. 2 (2015) 57.
[167] D. Xiao, W. Yao, Q. Niu, Valley-contrasting physics in graphene: magnetic moment and topological transport, Phys. Rev. Lett. 99 (2007), 236809.
[168] W. Yao, D. Xiao, Q. Niu, Valley-dependent optoelectronics from inversion symmetry breaking, Phys. Rev. B 77 (2008), 235406.
[169] G. Wang, A. Chernikov, M.M. Glazov, T.F. Heinz, X. Marie, T. Amand, B. Urbaszek, Colloquium: Excitons in atomically thin transition metal dichalcogenides, Rev. Mod. Phys. 90 (2018), 021001.
[170] K. Kośmider, J.W. González, J. Fernández-Rossier, Large spin splitting in the conduction band of transition metal dichalcogenide monolayers, Phys. Rev. B 88 (2013), 245436.
[171] E. Tang, J.W. Mei, X.G. Wen, High-temperature fractional quantum Hall states, Phys. Rev. Lett. 106 (2011), 236802.
[172] K. Sun, Z. Gu, H. Katsura, S. Das Sarma, Nearly flatbands with nontrivial topology, Phys. Rev. Lett. 106 (2011), 236803.
[173] H. Katsura, I. Maruyama, A. Tanaka, H. Tasaki, Ferromagnetism in the Hubbard model with topological/non-topological flat bands, EPL (Europhysics Letters) 91 (2010) 57007.
[174] T. Neupert, L. Santos, C. Chamon, C. Mudry, Fractional quantum Hall states at zero magnetic field, Phys. Rev. Lett. 106 (2011), 236804.
[175] Z. Liu, Z.F. Wang, J.W. Mei, Y.S. Wu, F. Liu, Flat Chern band in a two-dimensional organometallic framework, Phys. Rev. Lett. 110 (2013), 106804.
[176] Z.F. Wang, N. Su, F. Liu, Prediction of a two-dimensional organic topological insulator, Nano Lett. 13 (2013) 2842.
[177] M. Zhou, Z. Liu, W. Ming, Z. Wang, F. Liu, sd^2 Graphene: Kagome band in a hexagonal lattice, Phys. Rev. Lett. 113 (2014), 236802.
[178] X. Zhang, M. Zhao, Robust half-metallicity and topological aspects in two-dimensional Cu-TPyB, Sci. Rep. 5 (2015) 14098.
[179] O.J. Silveira, S.S. Alexandre, H. Chacham, Electron states of 2D metal-organic and covalent-organic honeycomb frameworks: ab initio results and a general fitting hamiltonian, J. Phys. Chem. C 120 (2016) 19796.
[180] M.G. Yamada, T. Soejima, N. Tsuji, D. Hirai, M. Dincă, H. Aoki, First-principles design of a half-filled flat band of the kagome lattice in two-dimensional metal-organic frameworks, Phys. Rev. B 94 (2016) 081102(R).
[181] L.Z. Zhang, Z.F. Wang, B. Huang, B. Cui, Z. Wang, S.X. Du, H.J. Gao, F. Liu, Intrinsic two-dimensional organic topological insulators in metal-dicyanoanthracene lattices, Nano Lett. 16 (2016) 2072.
[182] Z. Li, J. Zhuang, L. Wang, H. Feng, Q. Gao, X. Xu, W. Hao, X. Wang, C. Zhang, K. Wu, S.X. Dou, L. Chen, Z. Hu, Y. Du, Realization of flat band with possible nontrivial topology in electronic Kagome lattice, Sci. Adv. 4 (2018) eaau4511.
[183] X. Zhang, Z. Wang, M. Zhao, F. Liu, Tunable topological states in electron-doped HTT-Pt, Phys. Rev. B 93 (2016), 165401.
[184] O.J. Silveira, H. Chacham, Electronic and spin-orbit properties of the kagome MOF family M_3(1,2,5,6,9,10-triphenylenehexathiol)$_2$ (M = Ni, Pt, Cu and Au), J. Phys. Condens. Matter 29 (2017) 09LT01.
[185] R. Dong, M. Pfeffermann, H. Liang, Z. Zheng, X. Zhu, J. Zhang, X. Feng, Large-area, free-standing, two-dimensional supramolecular polymer single-layer sheets for highly efficient electrocatalytic hydrogen evolution, Angew. Chem. Int. Ed. 54 (2015) 12058.
[186] H. Liu, G. Sethi, D.N. Sheng, Y. Zhou, J.-T. Sun, S. Meng, F. Liu, High-temperature fractional quantum Hall state in the Floquet kagome flat band, Phys. Rev. B 105 (2022), L161108.
[187] C.H. Lee, M. Claassen, R. Thomale, Band structure engineering of ideal fractional Chern insulators, Phys. Rev. B 96 (2017), 165150.
[188] R. Morf, B.I. Halperin, Monte Carlo evaluation of trial wavefunctions for the fractional quantized hall effect: spherical geometry, Z. Phys. B 68 (1987) 391.
[189] R.L. Willett, H.L. Stormer, D.C. Tsui, A.C. Gossard, J.H. English, Quantitative experimental test for the theoretical gap energies in the fractional quantum Hall effect, Phys. Rev. B 37 (1988) 8476.
[190] I.V. Savochkin, A.K. Zvezdin, V.I. Belotelov, Optically pumped Floquet states of magnetization in ferromagnets, Opt. Lett. 44 (2019) 331.
[191] X. Liu, P. Tang, H. Hübener, U. D. Giovannini, W. Duan, and A. Rubio, Floquet Engineering of Magnetism in Topological Insulator Thin Films. arXiv: 2106.06977.
[192] Y. Murakami, M. Eckstein, P. Werner, Floquet DMFT analysis of high harmonic generation in mott insulators, JPS Conf. Proc. 30 (2020), 011183.
[193] J. Liu, K. Hejazi, L. Balents, Floquet engineering of multiorbital mott insulators: applications to orthorhombic titanates, Phys. Rev. Lett. 121 (2018), 107201.
[194] K.I. Seetharam, C.-E. Bardyn, N.H. Lindner, M.S. Rudner, G. Refael, Steady states of interacting Floquet insulators, Phys. Rev. B 99 (2019), 014307.
[195] D.M. Kennes, A.d.l. Torre, A. Ron, D. Hsieh, A.J. Millis, Floquet Engineering in Quantum Chains, Phys. Rev. Lett. 120 (2018) 127601.
[196] S. Fazzini, P. Chudzinski, C. Dauer, I. Schneider, S. Eggert, Nonequilibrium floquet steady states of time-periodic driven luttinger liquids, Phys. Rev. Lett. 126 (2021), 243401.
[197] A. Li, M. Reutzel, Z. Wang, D. Novko, B. Gumhalter, H. Petek, Plasmonic photoemission from single-crystalline silver, ACS Photonics 8 (2021) 247.
[198] D. Novko, V. Despoja, M. Reutzel, A. Li, H. Petek, B. Gumhalter, Plasmonically assisted channels of photoemission from metals, Phys. Rev. B 103 (2021), 205401.
[199] N. Tsuji, T. Oka, H. Aoki, Correlated electron systems periodically driven out of equilibrium: Floquet + DMFT formalism, Phys. Rev. B 78 (2008), 235124.
[200] A. Lerose, M. Sonner, D.A. Abanin, Influence matrix approach to many-body floquet dynamics, Phys. Rev. X 11 (2021), 021040.
[201] M. Bukov, M. Kolodrubetz, A. Polkovnikov, Schrieffer-Wolff transformation for periodically driven systems: strongly correlated systems with artificial gauge fields, Phys. Rev. Lett. 116 (2016), 125301.
[202] H.C. Po, L. Fidkowski, T. Morimoto, A.C. Potter, A. Vishwanath, Chiral floquet phases of many-body localized bosons, Phys. Rev. X 6 (2016), 041070.
[203] A.C. Potter, T. Morimoto, A. Vishwanath, Classification of interacting topological floquet phases in one dimension, Phys. Rev. X 6 (2016), 041001.
[204] M. Puviani, F. Manghi, Periodically driven interacting electrons in one dimension: Many-body Floquet approach, Phys. Rev. B 94 (2016) 161111(R).
[205] P. Titum, E. Berg, M.S. Rudner, G. Refael, N.H. Lindner, Anomalous floquet-anderson insulator as a nonadiabatic quantized charge pump, Phys. Rev. X 6 (2016), 021013.
[206] P. Liang, M. Marthaler, L. Guo, Floquet many-body engineering: topology and many-body physics in phase space lattices, New J. Phys. 20 (2018), 023043.
[207] K. Seetharam, P. Titum, M. Kolodrubetz, G. Refael, Absence of thermalization in finite isolated interacting Floquet systems, Phys. Rev. B 97 (2017), 014311.
[208] T. Qin, W. Hofstetter, Nonequilibrium steady states and resonant tunneling in time-periodically driven systems with interactions, Phys. Rev. B 97 (2018), 125115.
[209] S. Kitamura, T. Oka, H. Aoki, Probing and controlling spin chirality in Mott insulators by circularly polarized laser, Phys. Rev. B 96 (2017), 014406.
[210] R. Moessner, S.L. Sondhi, Equilibration and order in quantum Floquet matter, Nat. Phys. 13 (2017) 424.
[211] P. Bordia, H. Luschen, U. Schneider, M. Knap, I. Bloch, Periodically driving a many-body localized quantum system, Nat. Phys. 13 (2017) 460.
[212] M. Claassen, H.C. Jiang, B. Moritz, T.P. Devereaux, Dynamical time-reversal symmetry breaking and photo-induced chiral spin liquids in frustrated Mott insulators, Nat. Commun. 8 (2017) 1192.
[213] F. Harper, R. Roy, Floquet topological order in interacting systems of bosons and fermions, Phys. Rev. Lett. 118 (2017), 115301.
[214] K. Takasan, M. Nakagawa, N. Kawakami, Laser-irradiated Kondo insulators: Controlling the Kondo effect and topological phases, Phys. Rev. B 96 (2017), 115120.
[215] D. Reiss, F. Harper, R. Roy, Interacting Floquet topological phases in three dimensions, Phys. Rev. B 98 (2018), 045127.
[216] G.S. Uhrig, M.H. Kalthoff, J.K. Freericks, Positivity of the spectral densities of retarded floquet green functions, Phys. Rev. Lett. 122 (2019), 130604.
[217] K.S.C. Decker, C. Karrasch, J. Eisert, D.M. Kennes, Floquet engineering topological many-body localized systems, Phys. Rev. Lett. 124 (2020), 190601.
[218] F.J. Garcia-Vidal, C. Ciuti, T.W. Ebbesen, Manipulating matter by strong coupling to vacuum fields, Science 373 (2021), eabd0336.
[219] J. Feist, Hybrid light–matter states in self-assembling cavities, Nature 597 (2021) 185.
[220] A. Frisk Kockum, A. Miranowicz, S. De Liberato, S. Savasta, F. Nori, Ultrastrong coupling between light and matter, Nat. Rev. Phys. 1 (2019) 19.
[221] J. Bloch, A. Cavalleri, V. Galitski, M. Hafezi, A. Rubio, Strongly correlated electron-photon systems, Nature 606 (2022) 41.
[222] J. Flick, M. Ruggenthaler, H. Appel, A. Rubio, Atoms and molecules in cavities, from weak to strong coupling in quantum-electrodynamics (QED) chemistry, Proc. Natl. Acad. Sci. U. S. A. 114 (2017) 3026.
[223] C. Genet, J. Faist, T.W. Ebbesen, Inducing new material properties with hybrid light–matter states, Phys. Today 74 (2021) 42.

[224] T. Karzig, C.-E. Bardyn, N.H. Lindner, G. Refael, Topological polaritons, *Phys. Rev. X* 5 (2015), 031001.
[225] H. Hubener, U. De Giovannini, C. Schafer, J. Andberger, M. Ruggenthaler, J. Faist, A. Rubio, Engineering quantum materials with chiral optical cavities, Nat. Mater. 20 (2021) 438.
[226] T.W. Ebbesen, Hybrid light-matter states in a molecular and material science perspective, Acc. Chem. Res. 49 (2016) 2403.
[227] F. Appugliese, J. Enkner, G.L. Paravicini-Bagliani, M. Beck, C. Reichl, W. Wegscheider, G. Scalari, C. Ciuti, J. Faist, Breakdown of topological protection by cavity vacuum fields in the integer quantum Hall effect, Science 375 (2022) 1030.
[228] Z. Sun, J. Gu, A. Ghazaryan, Z. Shotan, C.R. Considine, M. Dollar, B. Chakraborty, X. Liu, P. Ghaemi, S. Kéna-Cohen, V.M. Menon, Optical control of room-temperature valley polaritons, Nat. Photonics 11 (2017) 491.
[229] M.A. Sentef, M. Ruggenthaler, A. Rubio, Cavity quantum-electrodynamical polaritonically enhanced electron-phonon coupling and its influence on superconductivity, Sci. Adv. 4 (2018), eaau6969.
[230] H. Gao, F. Schlawin, M. Buzzi, A. Cavalleri, D. Jaksch, Photoinduced electron pairing in a driven cavity, Phys. Rev. Lett. 125 (2020), 053602.
[231] Y. Dai, A. Ghosh, S. Yang, Z. Zhou, C.-B. Huang, H. Petek, Poincaré engineering of surface plasmon polaritons, Nat. Rev. Phys. 4 (2022) 562.
[232] A. Forbes, M. de Oliveira, M.R. Dennis, Structured light, Nat. Photonics 15 (2021) 253.
[233] Y. Dai, Z. Zhou, A. Ghosh, K. Kapoor, M. Dąbrowski, A. Kubo, C.-B. Huang, H. Petek, Ultrafast microscopy of a twisted plasmonic spin skyrmion, Appl. Phys. Rev. 9 (2022), 011420.
[234] A. Sekine, K. Nomura, Axion electrodynamics in topological materials, J. Appl. Phys. 129 (2021), 141101.
[235] D.M. Nenno, C.A.C. Garcia, J. Gooth, C. Felser, P. Narang, Axion physics in condensed-matter systems, Nat. Rev. Phys. 2 (2020) 682.
[236] A. Kirilyuk, A.V. Kimel, T. Rasing, Ultrafast optical manipulation of magnetic order, Rev. Mod. Phys. 82 (2010) 2731.